Assessment of Natural Gas Pipeline Construction on Stream Temperature and Turbidity in Southwestern Virginia, 2017—25

By Brendan M. Foster, Carly M. Maas, and Alejandra L. Flota

Acknowledgments

The authors wish to thank the numerous U.S. Geological Survey (USGS) staff that have contributed to the design, maintenance, and operation of this study since 2017. Technical reviews by Samuel Miller and Spencer Tassone of the USGS strengthened the report and their comments are greatly appreciated.

Outline

Acknowledgments
Introduction
- Description of Study Area
- Overview of Pipeline Construction
- Monitoring Site Selection
- Purpose and Scope

Methods of Investigation
- Monitoring Design
- Real-time Alert Application
- Statistical Analysis of Water Temperature and Turbidity
  - Continued Statistical Analysis of Water Temperature
    - Water Temperature Anomaly Detection
  - Continued Statistical Analysis of Turbidity
    - Stormflow Hysteresis

Spatial and Temporal Patterns of Water Temperature
- Comparative Analysis of Upstream and Downstream Water Temperature Conditions
- Detection of Water Temperature Anomalies
- Discussion of Water Temperature Results

Short- and Long- Term Patterns of Turbidity
- Turbidity Conditions and Comparison of Upstream versus Downstream Stations
- Storm Hysteresis Patterns of Turbidity
- Discussion of Turbidity Results

Utility of Real-Time Alert Application
Summary
References Cited
Appendix 1. Supporting Material for Turbidity Analysis

Figures

Figure 1. Map showing U.S. Geological Survey water-quality and gage height monitoring stations along the Mountain Valley Pipeline (MVP) in southwestern Virginia. Stations names are defined in Table 1.
Figure 2. Maps showing aerial upstream and downstream monitoring locations compared to the pipeline construction. *A,* Little Stony Creek; *B,* Sinking Creek; *C,* Roanoke River; *D,* Upper Bottom Creek; *E,* Lower Bottom Creek; *F.* Blackwater River.
Figure 3. Time series of the hourly median water temperature. Vertical dashed lines indicate the during crossing construction period. *A.* Time series of the upstream and downstream sites for each paired station, *B.* Time series of the downstream – upstream and the identified temperature anomalies when seasonality and long-term trends were removed.
Figure 4. Scatterplot of each paired station in the before, during, and after period. The 1-to-1 golden dashed line represents when the upstream and downstream hourly median temperatures are equivalent. *A.* Little Stony Creek; *B.* Sinking Creek; *C.* Roanoke River; *D.* Upper Bottom Creek, *E.* Lower Bottom Creek, *F.* Blackwater River.
Figure 5. Scatterplot of the hourly median temperature difference of the anomalies and the duration, in hours, of the anomalies in the before, during, and after period. *A.* Little Stony Creek; *B.* Sinking Creek; *C.* Roanoke River; *D.* Upper Bottom Creek, *E.* Lower Bottom Creek, *F.* Blackwater River.
Figure 6. High-frequency turbidity and gage height time series at Lower Bottom Creek in the before crossing, during crossing, and after crossing periods. *A,* Gage Height at Downstream Lower Bottom Creek; *B.* Turbidity at the Upstream and downstream Lower Bottom Creek; *C,* Turbidity in the during crossing period.
Figure 7. Hourly median turbidity at downstream station versus upstream station in the before, during, and after period. The golden dashed line is a 1-to-1 line.
Figure 8. Histograms showing the baseflow turbidity differences between the upstream and the downstream site in the before, during, and after crossing period compared to the frequency of observations. A positive turbidity indicates the downstream turbidity was higher and a negative turbidity indicates the upstream turbidity was higher.
Figure 9. Graph showing the relations of median hysteresis index to median slope of the upstream and downstream site at all 6 crossing locations, *A,* Before Crossing; *B,* During Crossing; *C,* After Crossing. A positive median hysteresis index indicates rapid delivery and negative is delayed delivery. Positive median slope is transport-limited, and a negative median slope is supply limited.
Figure 1.1. High-frequency time series of the before crossing, during crossing, and after crossing period. *A,* Little Stony Creek turbidity at the upstream and downstream site; *B,* Gage height at Little Stony Creek downstream site; *C,* Sinking Creek turbidity at the upstream and downstream site; *D,* Gage height at Sinking Creek upstream site.
Figure 1.2. High-frequency time series of the before crossing, during crossing, and after crossing period. *A,* Roanoke River turbidity at the upstream and downstream site; *B,* Gage height at Roanoke River Lafayette monitoring station upstream of upstream site; *C,* Upper Bottom Creek turbidity at the upstream and downstream site; *D,* Gage height at Upper Bottom Creek downstream site.
Figure 1.3. High-frequency time series of the before crossing, during crossing, and after crossing period. *A,* Lower Bottom Creek turbidity at the upstream and downstream site; *B,* Gage height at Lower Bottom Creek in the downstream site; *C,* Blackwater River turbidity at the upstream and downstream site; *D,* Gage height at Blackwater River downstream site.

Figure 1.4. Graphs of the hysteresis index and slope. *A,* Before Crossing at Upstream Sites; *B,* During Crossing at Upstream Sites; *C,* After Crossing at Upstream sites; *D,* Before Crossing at Downstream Sites; *E,* During Crossing at Downstream Sites; *F,* After Crossing at Downstream Sites.

TablesU.S. customary units to International System of Units
International System of Units to U.S. customary units
Table 1. Description of the 13 U.S. Geological Survey water quality monitoring stations.
Table 2. Description of the Mountain Valley Pipeline stream crossing methods and timeline in southwestern, Virginia. The before period began at the start of monitoring and ended a day before the start of construction, the during period began at the start of construction and ended at the end of construction, and the after period began a day after the end of construction through the end of the monitoring. The upstream and downstream distance from the ROW (ft) was calculated as the length along the stream.
Table 3. Description of the thresholds used for the real-time alert application. Baseline turbidity is the maximum of the median turbidities across upstream and downstream gages through a 24-hour period.
Table 4. Characterization of the distribution of the high-frequency (5-minute interval) data of water temperature at all sites throughout the before crossing, during crossing, and after crossing construction.
Table 5. Results of the bootstrapped hourly median differences between the upstream and downstream time-matched paired turbidity observation during stormflow in the before, during, and after crossing period. A negative median temperature, lower 99-percent confidence interval, and upper 99-percent confidence interval indicates that the upstream site was warmer than the downstream site and a positive temperature value indicates that the downstream site was warmer than the upstream.
Table 6. Descriptive statistics of turbidity for each site, station and period. Statistics were calculated using the raw 5-minute interval data and include N, number of observations; Min, minimum value; Q1, first quartile; Median, median value; Q3, third quartile; and Max, maximum value.
Table 7. Results of the bootstrapped median of hourly median differences between the upstream and downstream time-matched paired turbidity observation in the before, during, and after crossing period.
Table 8. Summary of the number of flags from January 2018 to June 2025 by field parameter using the real-time alert application.
Table 1.1. Number and percentage of values censored that were greater than 1000 FNU.
Table 1.2. Results of the percentage of absolute differences for each time-matched paired hourly median turbidity measurements between the upstream and downstream for each site and period.

Conversion Factors

U.S. customary units to International System of Units

Multiply	By	To obtain
	Length	
inch (in.)	2.54	centimeter (cm)
inch (in.)	25.4	millimeter (mm)
foot (ft)	0.3048	meter (m)
mile (mi)	1.609	kilometer (km)
	Area	
section (640 acres or 1 square mile)	259.0	square hectometer (hm^2)
square mile (mi^2)	259.0	hectare (ha)

Multiply	By	To obtain
square mile (mi^2)	2.590	square kilometer (km^2)
	Flow rate	
inch per hour (in/h)	0.0254	meter per hour (m/h)
inch per year (in/yr)	25.4	millimeter per year (mm/yr)
mile per hour (mi/h)	1.609	kilometer per hour (km/h)

International System of Units to U.S. customary units

Multiply	By	To obtain
	Length	
centimeter (cm)	0.3937	inch (in.)
millimeter (mm)	0.03937	inch (in.)
meter (m)	3.281	foot (ft)
kilometer (km)	0.6214	mile (mi)
	Area	
square hectometer (hm^2)	0.003861	section (640 acres or 1 square mile)
hectare (ha)	0.003861	square mile (mi^2)
square kilometer (km^2)	0.3861	square mile (mi^2)
	Flow rate	
millimeter per year (mm/yr)	0.03937	inch per year (in/yr)

Temperature in degrees Celsius (°C) may be converted to degrees Fahrenheit (°F) as follows:

°F = (1.8 × °C) + 32.

Temperature in degrees Fahrenheit (°F) may be converted to degrees Celsius (°C) as follows:

°C = (°F – 32) / 1.8.

Datums

Vertical coordinate information is referenced to the North American Vertical Datum of 1988 (NAVD 88).

Horizontal coordinate information is referenced to the North American Datum of 1983 (NAD 83).

Elevation, as used in this report, refers to distance above the vertical datum.

Supplemental Information

Specific conductance is in microsiemens per centimeter at 25 degrees Celsius (µS/cm at 25 °C).

Turbidity is in Formazin Nephelometric Units (FNU)

Dissolved oxygen is in milligrams per liter

A water year is the 12-month period from October 1 through September 30 of the following year and is designated by the calendar year in which it ends.

Abbreviations

CI	confidence interval
DEQ	Virginia Department of Environmental Quality
HI	hysteresis index
LOESS	locally estimated scatterplot smoothing
MVP	Mountain Valley Pipeline
NHST	null hypothesis statistical tests
Q1	first quartile
Q3	third quartile
ROW	right-of-way
SC	specific conductance
STL	seasonal and trend decomposition using LOESS
TB	turbidity
Transco	Transcontinental Gas Pipe Line Company, LLC
USGS	U.S. Geological Survey
WT	water temperature

Abstract

The natural gas pipeline network in the United States is extensive and often intersects streams and other sensitive habitats, yet there are limited case studies utilizing a comparative upstream-downstream approach to evaluate potential short- and long-term effects of pipeline stream crossing construction from pre-construction to post-site restoration. In 2017, the U.S. Geological Survey, in cooperation with the Virginia Department of Environmental Quality (DEQ), deployed real-time continuous stream monitoring stations upstream and downstream of six proposed Mountain Valley Pipeline (MVP) stream crossings in southwestern Virginia. Water temperature and turbidity data collected at the upstream and downstream sites were compared across three periods – before crossing construction, during crossing construction, and after crossing construction – to elucidate potential impacts from the stream crossing construction. Additionally, the monitoring network was utilized to notify regulators of potentially anomalous conditions throughout the entire monitoring period.

Results of this study indicate (1) at all six monitored streams, pipeline stream crossing construction did not affect long-term or short-term upstream-to-downstream water temperature conditions; (2) pipeline stream crossing construction did not affect long-term upstream-to-downstream turbidity conditions in all six monitored streams. Some short-term anomalously elevated turbidity conditions were observed and attributable to pipeline stream crossing construction; however, the duration and magnitude were not sufficient to alter the long-term turbidity regime of the streams in which they were observed; and (3) the application of the monitoring network as a real-time alert system successfully alerted regulators to potentially anomalous conditions.

Introduction

The natural gas pipeline network in the United States extends over three million miles, reliably serving 78.5 million people and providing electric power generation, industrial applications, residential needs, commercial activities, and transportation (U.S. Energy Information Administration, 2024a; U.S. Energy Information Administration, 2024b). At of the beginning of 2024, a total of 122,552 miles of pipeline were either under construction or in the planning stages worldwide (Reed, 2024). During construction, pipelines can traverse sensitive aquatic habitats critical to both wildlife and human activities, potentially jeopardizing the ecosystem and resources affected by pipeline crossing operations (Castro and others, 2015). Therefore, an in-depth understanding of the potential short- and long- term effects of pipeline stream crossing construction—such as changes in water temperature regimes or sedimentation—on streams, particularly those with sensitive habitats, ecosystems, and natural resources, is imperative.

There are few studies which investigate the potential short- and long-term impacts of pipeline construction on streams. Potential impacts include increases in turbidity and suspended sediment, modification of stream habitat, and pollutants entering stream in the event of equipment failures or spills and on a longer time scale can lead to stream channel incision and lateral migration (Castro and others, 2015). Increased suspended sediment can impact biota directly by reducing light required for photosynthesis, burying habitat, and transporting particle-associated contaminates (Moyer and Hyer, 2009; Miller and others, 2023). During construction, suspended sediment could enter the stream through exaction and backfilling trenches, erosion from upland construction, and discharge of water from hydrostatic pipe testing or trench dewatering (Moyer and Hyer, 2009). A case study on the Jewell Pipeline in the Appalachian

Mountains of Virginia monitored turbidity as a proxy for suspended sediment concentrations and found small increases in turbidity during the construction (Moyer and Hyer, 2009). While there is not currently any regulation on turbidity in Virginia, excess sediment is a common reason that water bodies can be listed as impaired (Miller and others, 2023).

Water temperature (WT) is a key state variable that directly and indirectly influences stream physical, chemical, and biological processes (Bonacina and others, 2023; van Hamel and Brunner, 2024; Johnson and others, 2024; Leach and others, 2023). Some of these processes include the solubility of dissolved oxygen, toxicity of chemicals, pH, the density of water, organic matter degradation, microbial metabolic activity, and primary production (Bonacina and others, 2023). In Virginia, there are regulations in place for water temperature in surface water bodies (Virginia Administrative Code 9VAC25-260-50). Although water temperature is a vital factor in stream health, few studies have examined potential changes in water temperature from pipeline construction. Of the pipeline crossing studies that have considered water temperature, all have provided evidence that water temperature was not affected by construction activities (Gowdy and others, 1994; Houser and Pruess, 2009).

An over seven-year study conducted by the U.S. Geological Survey (USGS) in cooperation with the Virginia Department of Environmental Quality (DEQ) was designed to continuously monitor water-quality conditions at six Mountain Valley Pipeline (MVP) stream crossings. This report analyzes the high-frequency water temperature and turbidity time series before, during, and after the MVP stream crossing period. This analysis was conducted to directly assess the magnitude and duration of potential changes, if any, in sediment and water temperature conditions and determine if they were directly attributable to pipeline crossing construction.

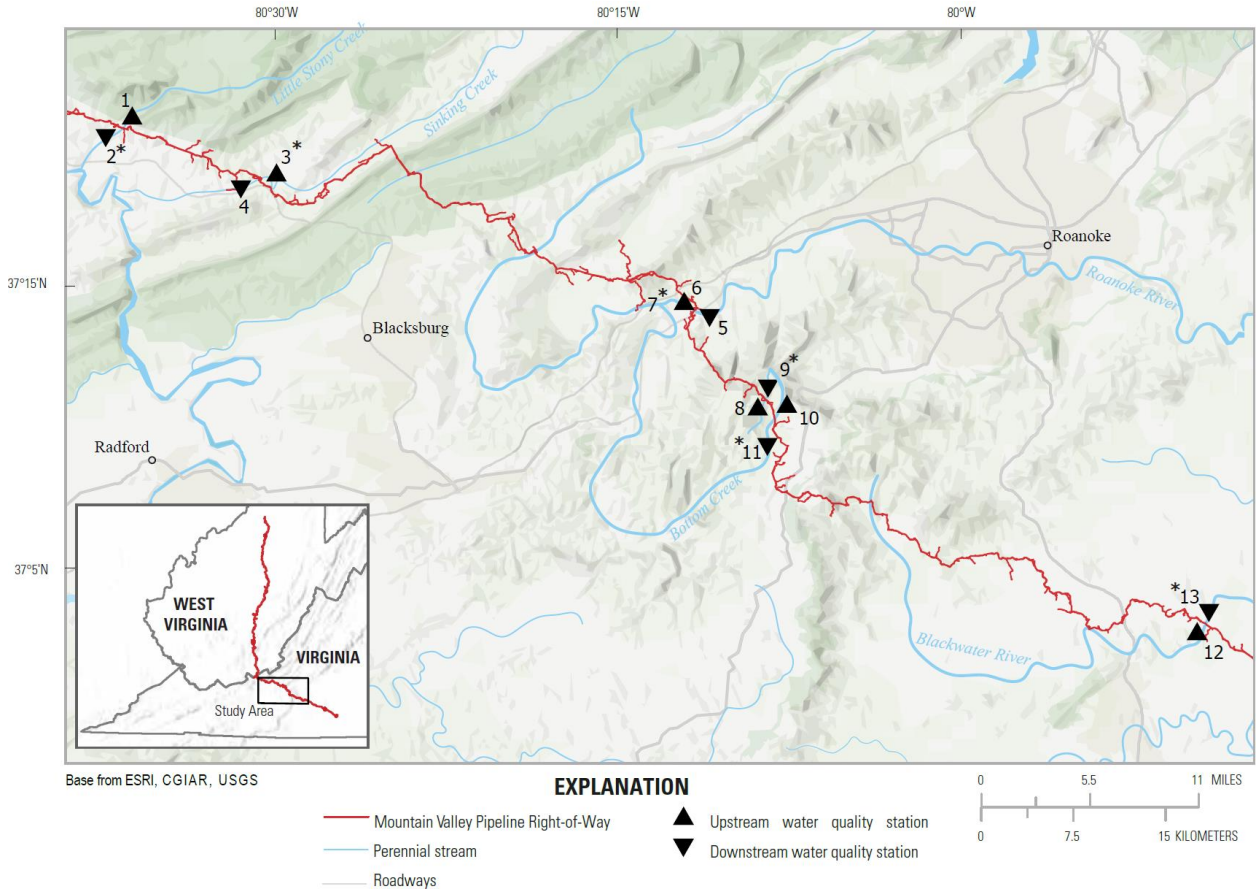

Figure 1. Map showing U.S. Geological Survey water-quality and gage height monitoring stations along the Mountain Valley Pipeline (MVP) in southwestern Virginia. Stations names are defined in Table 1.

Description of Study Area

The MVP is a natural gas transmission pipeline which originates in northwestern West Virginia and ends in south-central Virginia (Figure 1). The purpose of the pipeline is to connect West Virginia's Marcellus shale region near Wetzel County, West Virginia to the existing Transcontinental Gas Pipe Line Company, LLC (Transco) gas transmission pipeline in Pittsylvania County, Virginia (Parfomak and Vann, 2022). The 42-inch diameter pipeline spans approximately 303 miles and crosses the Appalachian Mountains. The pipeline was initially proposed in 2014 and construction began January 1, 2018 (Parfomak and Vann, 2024); however,

construction of the pipeline was suspended numerous times due to permitting issues in federal court. Construction was completed on June 10, 2024, and the MVP was approved to begin commercial service on June 11, 2024 (Parfomak and Vann, 2024).

The study sites are located in the Appalachian Basin and the Piedmont-Blue Ridge Physiographic Provinces, with varying topography of areas with high slope and highly erodible soils (Betcher and others, 2019; Lévesque and Dubé, 2007; New River Geographics, 2017; U.S. Geological Survey, 2025a). The karst topography in this region is characterized by vast caves and other subsurface water conduits and can pose an additional risk during construction activities (Lévesque and Dubé, 2007; Zerga, 2024).

The climate within this region is subtropical, characterized by mild summers and winters, with an annual average temperature of 14.2 degrees Celsius (°C) (Roanoke Weather Records, 2025). Roanoke, Virginia (located approximately in the middle of the study area) receives an average annual rainfall of 42.8 inches and average snowfall of 14.7 in (Coats and Jackson, 2020; Roanoke Weather Records, 2025). This study area is predominantly deciduous, coniferous, and mixed forest, comprised of northern hardwood, cove hardwood, and mixed deciduous trees (Turner and others, 2003; Virginia Department of Conservation and Recreation, 2021). Mature trees in this region have an average height of 100 feet, providing dense canopy cover across the mountain range (Coats and Jackson, 2020).

Overview of Pipeline Construction

MVP intersects approximately 139 streams and 61 wetlands across Virginia and West Virginia, primarily in rural and previously undisturbed areas (Betcher and others, 2019; Downstream Strategies and West Virginia Rivers, 2024). Various stream crossing methods were

utilized during the construction, which are summarized in this report as either trenched or trenchless crossings. Stream crossing methods were selected based on the characteristics of the landscape, including stream width, the steepness of the adjacent slopes, local geology, available space for construction activities, and proximity to residential areas, roads, or environmental resources (Tetra Tech, 2021).

The trenched crossing method used was a conventional dry-ditch open cut method (Tetra Tech, 2021). Trenched crossing methods isolate the construction site by diverting streamflow to dry or nearly dry conditions using a temporary coffer dam (Castro and others, 2015; Reid and others, 2002). The workflow includes excavating the trench, installing the pipe in the trench, and backfilling the trench. Trenched methods may disrupt sediment during installation and after removal of the dam (Lévesque and Dubé, 2007; Reid and others, 2002).

Trenchless methods install the pipeline by drilling boreholes beneath the stream, completing the installation without disturbing the surface or streambed (Castro and others, 2015; New Jersey Department of Environmental Protection, 2021; Yan and others, 2018). The pipeline is installed as an arc beneath the stream and can often be several feet below the streambed (Castro and others, 2015). The suitable entry and exit locations for the pipeline may be identified outside of the streambank margins (Castro and others, 2015). Entry and exit points are initially drilled as a pilot hole by a drill rig, then drilling fluids are utilized to transport drill cuttings to the surface, maintain the borehole stability, and cool the drill bit (Yan and others, 2018). Trenchless methods for stream crossings can avoid the aquatic risks by boring outside the streambanks and underneath the stream, which is particularly used in sensitive or urban areas (Castro and others, 2015). However, there are associated risks with this approach as well, including groundwater infiltration and disruption of underground stream networks.

The pipeline requires both a temporary and permanent right of way (ROW) to accommodate construction and maintenance vehicles, equipment, and material stockpiles (Tetra Tech, 2021). In the upland areas, a 125-foot-wide construction ROW and 50-foot-wide permanent ROW were constructed (Tetra Tech, 2021). Within 50 feet of an aquatic resource crossing, the construction ROW narrows to 75 feet to preserve the riparian buffer (Tetra Tech, 2021).

After the sites were backfilled and hydrostatic tested, cleanup and restoration were completed. These activities include restoring the grade cuts to pre-construction topography and ground cover to regrow native plants, minimizing erosion, and stabilizing stream banks (Tetra Tech, 2021).

Monitoring Site Selection

The USGS monitored six perennial streams in cooperation with the Virginia DEQ along the MVP. These sites were selected based on the presence of threatened or endangered species, proximity to- or designation as- Virginia Tier III waters (Exceptional State Waters), high ecological integrity based on previous aquatic community, habitat and water quality surveys conducted by DEQ, public water supplies, upland construction areas, site access, and suitable water flow (Virginia Administrative Code 9VAC25-260-30). The monitoring sites varied in watershed area, elevation, and proximity to the pipeline crossing construction (Figure 2; Table 1).

The three smallest watersheds, Little Stony Creek, upper Bottom Creek, and lower Bottom Creek, all contain sections designated as Exceptional State Waters and are noted for wild trout populations, diverse benthic macroinvertebrate communities, and high-quality in-stream

and riparian habitat conditions (Virginia Administrative Code 9VAC25-260-30; Burton and Gerritsen, 2003; J. Hill, DEQ – Blue Ridge Regional Office, oral commun., 2017). This designation identifies, maintains, and protects the waterbody from permanent or long-term degradation (Virginia Administrative Code 9VAC25-260-30). Sinking Creek, the third largest watershed, is distinguished by both the high benthic macroinvertebrate diversity and the karstic geology. Upper Bottom Creek was crossed using trenched methods and Little Stony Creek, lower Bottom Creek, and Sinking Creek were crossed using trenchless methods.

The two largest watersheds, Blackwater River and Roanoke River, are prominent western Piedmont streams and are the water sources for Smith Mountain Lake, a reservoir used for drinking water and recreation by thousands of residents and visitors each year. Although the Blackwater River has a smaller watershed, it features two pipeline crossings within the study area – one on the tributary, Maggodee Creek, upstream of the monitoring area and another located between the two monitoring stations on the Blackwater River. Roanoke River serves as a vital public water supply for the City of Roanoke, Roanoke County, and the City of Salem in Virginia. Although the Roanoke River was crossed using trenchless methods and Blackwater River was crossed using trenched methods, the pipeline at both locations was installed at a minimum depth of six feet below the streambed (Tetra Tech, 2021).

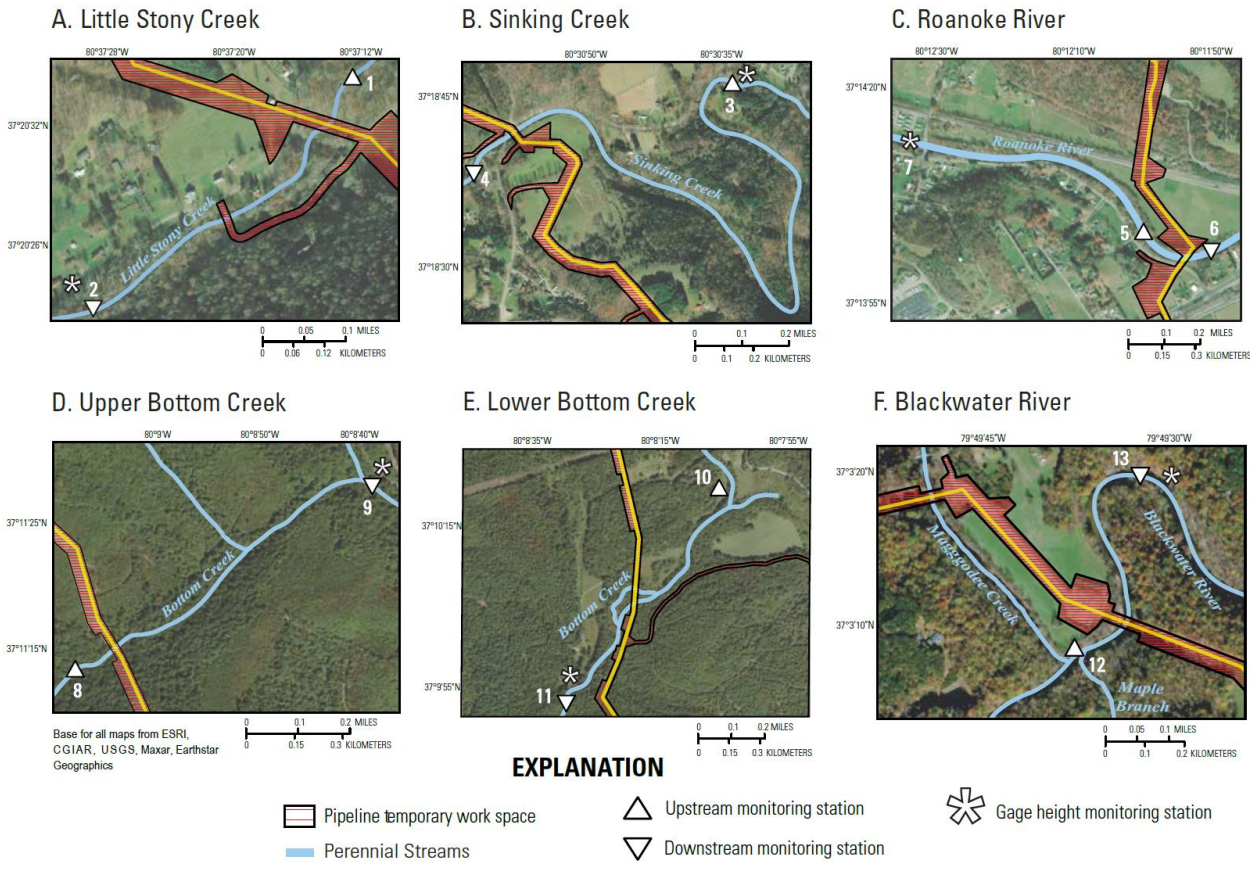

Figure 2. Maps showing aerial upstream and downstream monitoring locations compared to the pipeline construction. *A,* Little Stony Creek; *B,* Sinking Creek; *C,* Roanoke River; *D,* upper Bottom Creek; *E,* lower Bottom Creek; *F,* Blackwater River. Stations names are defined in Table 1.

Table 1. Description of the 13 U.S. Geological Survey water quality monitoring stations (U.S. Geological Survey, 2025b).

[Site numbers are shown on Figure 1. no. number; ID, identifier; USGS, U.S. Geological Survey; *, Sites with gage height; ft, feet; mi^2, square-miles]

Site No.	DEQ Site ID	USGS site number	USGS site name	Abbreviated site name	Latitude	Longitude	Elevation (ft)	Watershed area (mi^2)
1	9-LRY002.87	03171597	Little Stony Creek Above Archer Trail Near Pembroke, VA	Little Stony Creek upstream	37.343154	-80.619545	1,929	19.7
2	9-LRY002.87	0317159760	Little Stony Creek Below Archer Trail Near Pembroke, VA	Little Stony Creek downstream*	37.339560	-80.624550	1,906	20.2
3	9-LRY002.39	0317154954	Sinking Creek Along Route 604 Near Newport, VA	Sinking Creek upstream*	37.312663	-80.507729	1,876	65.2
4	9-SNK009.56	0317155123	Sinking Creek at Covered Bridge Ln Near Newport, VA	Sinking Creek downstream	37.310988	-80.516938	1,811	66.2
5	9-SNK008.19	0205450393	Roanoke River Along Route 626 at Lafayette, VA	Roanoke River upstream	37.234300	-80.199740	1,177	256
6	4AROA226.86	0205450495	Roanoke River Above Route 11 at Lafayette, VA	Roanoke River downstream	37.234630	-80.193080	1,184	257
7	4AROA226.86	02054500	Roanoke River at Lafayette, VA	Roanoke River gage height*	37.236527	-80.2092089	1,174	254
8	4AROA226.64	0205373035	Bottom Creek Above Tributary Near Bent Mountain, VA	Upper Bottom Creek upstream	37.187090	-80.151910	3,162	0.4
9	NA	0205373075	Bottom Creek Along Route 612 Near Bent Mountain, VA	Upper Bottom Creek downstream*	37.191370	-80.144080	3,024	0.98
10	4ABTM012.47	0205373228	Bottom Creek Above Confluence Near Bent Mountain, VA	Lower Bottom Creek upstream	37.173110	-80.135090	2,732	2.08
11	4ABTM011.94	0205373422	Bottom Creek Below Poor Mountain Near Bent Mountain, VA	Lower Bottom Creek downstream*	37.164750	-80.141360	2,693	3.44
12	4ABTM010.26	0205696042	Blackwater River Above Maple Branch Near Redwood, VA	Blackwater River upstream	37.052280	-79.826830	874	164
13	4ABTM009.25	0205696095	Blackwater River Below Maple Branch Near Redwood, VA	Blackwater River downstream*	37.052317	-79.826867	915	165

Purpose and Scope

The purpose of this report is to assess whether water temperature and turbidity regimes were affected by pipeline stream-crossing construction and to evaluate the utility of real-time stream monitoring alert networks during pipeline construction. These objectives were addressed through the following questions:

- Were there significant short-term or long-term anomalous water temperature or turbidity conditions in relation to pipeline stream crossing construction?
- Can stream monitoring networks be used to identify compliance alerts throughout pipeline construction?

The analysis herein is limited to answering the above-described questions specifically for the six monitored streams reaches. Potential construction-related anomalous conditions outside those specifically evaluated are possible but fall outside the scope of this report. Additionally, the study design and analysis address potential reach-specific effects only – potential overall or watershed-wide effects of pipeline construction are not evaluated from monitored data in this report.

Methods of Investigation

The interpretations presented in this report are derived from time series of continuous water-quality and water-level sensors placed upstream and downstream of natural gas pipeline stream crossings. These data were analyzed to evaluate short- and long-term water-temperature and turbidity conditions and the utility of this monitoring as a real-time alert application.

Monitoring Design

The continuous water-quality and water-level monitoring network for the MVP was established at six pipeline stream crossings in 2017 (Figure 1). Each site had a paired monitoring design, with stations upstream and downstream of the pipeline stream crossing. Watershed areas spanned from less than 1 mi^2 to 260 mi^2 (Table 1). Paired monitoring stations were used to assess downstream changes in water temperature and turbidity relative to the upstream conditions. Water levels were measured at one station per site, except for the Roanoke River, where water level measurements were taken at upstream USGS gage 02054500 (Table 1). Data were reported in near real-time to support and inform the real-time alert application.

Data were analyzed to assess water temperature and turbidity conditions before, during, and after pipeline crossing construction (Table 2). The “before” period includes all dates from the establishment of the monitoring station up to the day prior to stream crossing construction (2,123 to 2,289 days). Due to intermittent construction caused by permitting issues, activities not associated with the stream crossing construction, such as tree clearing and ROW construction, are included in the before period. The “during” period includes the pipeline stream crossing construction and the immediate post-crossing restoration work (12 to 208 days). The “after” period is at least one year post-stream crossing construction (366 to 595 days).

Table 2. Description of the Mountain Valley Pipeline stream crossing methods and timeline in southwestern, Virginia. The before period began at the start of monitoring and ended a day before the start of construction, the during period began at the start of construction and ended at the end of construction, and the after period began a day after the end of construction through the end of the monitoring. The upstream and downstream distances from the right-of-way (ROW) (in feet, ft) were calculated as the length along the stream.

[ft, feet]

Stream name	Crossing method	Upstream Distance from ROW (ft)	Downstream Distance from ROW (ft)	Total distance between upstream and downstream (ft)	Start of Monitoring	Start of Construction	End of Construction	End of monitoring	Construction period (days)
Little Stony Creek	Trenchless	315	1,672	1,987	2017-08-26	2023-12-11	2024-04-29	2025-04-30	141
Sinking Creek	Trenchless	6,004	430	6,434	2017-11-07	2023-11-02	2024-04-15	2025-04-30	166
Roanoke River	Trenchless	576	438	1,014	2017-08-23	2023-09-21	2024-04-15	2025-04-30	208
Upper Bottom Creek	Trenched	227	2,536	2,763	2017-10-31	2023-08-24	2023-09-13	2025-04-30	21
Lower Bottom Creek	Trenchless	2,340	1,591	3,931	2017-10-27	2023-11-02	2024-04-26	2025-04-30	177
Blackwater River	Trenched	382	1,266	1,648	2017-11-09	2024-02-15	2024-02-26	2025-04-30	12

Continuous water-quality data were measured using YSI, Inc. (Yellow Springs, Ohio) 6-series Multiparameter Water Quality Sondes at 5-minute intervals for water temperature, specific conductance, pH, dissolved oxygen, and turbidity. Water temperature has a measurement resolution of 0.01 °C and a measurement accuracy of plus or minus (±) 0.15 °C (YSI, 2012). The measurement resolution for turbidity is 0.1 Formazin Nephelometric Units (FNU) with an accuracy of ± 2% of a measurement or 0.3 FNU, whichever is greater. Water levels were also measured at 5-minute intervals at six monitored pipeline crossings using a TE Connectivity (Galway, Ireland) KSPI 500 transducer or OTT HydroMet (Kempten, Germany) PLS pressure transducer. Peak stage verification was accomplished with additional water level measurements with an Onset HOBO (Bourne, Massachusetts) water level data logger. This report focuses solely on water temperature, turbidity, and water-level data for the entire period of record. All data were collected, and quality assured in accordance with USGS Guidelines and standard procedures (Wagner and others, 2006; Sauer and Turnipseed, 2010). Turbidity measurements exceeding 1,000 FNU are outside the manufacturer's stated measurement range and were censored and treated as values greater than 1,000 FNU, impacting less than 0.15-percent of all measurements (Table 1.1). This small amount of right-censored turbidity data was inconsequential to the analytical methods used and described in the subsequent subsection of this report and to the purpose of understanding potentially anomalously high upstream-to-downstream differences. All data in this report are publicly available on the USGS Water Data for the Nation (U.S. Geological Survey, 2025b).

Real-time Alert Application

The monitoring network was used by DEQ as a real-time alert tool for regulators of the pipeline construction. From January of 2018 through April of 2025, water temperature, pH,

dissolved oxygen, turbidity, and specific conductance were evaluated in real-time using an automated script for potential anomalous conditions. A flag (that is, an alert provided by the automated data review system) occurred when water quality measurements were below the minimum values or above maximum values set by the thresholds defined in Table 3.

A field visit could lead to four response categories by DEQ:

(1) No Action Required by DEQ,

(2) Field complaint reviewed, no additional DEQ actions required,

(3) Issues were noticed during the follow-up investigation into a pollution complaint, but these were addressed in real time by the Responsible Party with no longer term actions needed, and

(4) Further action was required.

Table 3. Description of the thresholds used for the real-time alert application. Baseline turbidity is the maximum of the median turbidities across upstream and downstream U.S. Geological Survey (USGS) sites during a 24-hour period. Refer to Table 1 for additional information about USGS sites.

[*, Cited from Virginia Administrative Code 9VAC25-260-50]

Field Parameter	Flag Name	Flag Definition
Water Temperature (WT)	Upstream maximum	Number of upstream WT (°C) samples exceeding maximum temperature standards*
	Downstream maximum	Number of downstream WT (°C) samples exceeding maximum temperature standards*
	Rise above natural	Number of times the difference between the upstream and downstream WT rose above natural temperature (1-3 °C depending on class*)
Dissolved Oxygen (DO)	Upstream minimum	Number of times upstream DO (mg/L) fell below the minimum DO standards*
	Downstream minimum	Number of times downstream DO (mg/L) fell below the minimum DO standards*
	Upstream-downstream difference	Number of times the difference between upstream and downstream DO was > 1 mg/L
pH	Upstream	Number of upstream pH samples that fell below or above the pH range standards*
	Downstream	Number of downstream pH samples that fell below or above the pH range standards*
	Upstream-downstream difference	Number of times the difference between upstream and downstream pH was outside the normal range (between pH min and pH max)
Specific Conductance (SC)	Upstream maximum	Number of upstream SC (µS/cm) samples exceeding maximum specific conductivity designations developed for each USGS gage by regional biologists.
	Downstream maximum	Number of downstream SC (µS/cm) samples exceeding maximum specific conductivity designations developed for each USGS gage by DEQ regional biologists.
	Upstream-downstream difference	Number of times the difference between upstream and downstream SC (µS/cm) exceeded the difference threshold developed for each USGS gage by DEQ regional biologists.
	Upstream-downstream percentage difference	Number of times the percent difference between upstream and downstream SC (µS/cm) exceeded the percent difference threshold developed for each USGS gage by DEQ regional biologists.
Turbidity (TB)	Upstream-downstream exceedance	Number of 30-minute windows where downstream TB exceeded upstream by at least 6 FNU, for sites with a baseline TB ≤ 40 FNU.
	Upstream-downstream percentage exceedance	Number of 30-minute windows where downstream TB was at least 15% higher than upstream TB, for sites with a baseline TB > 40 FNU.
	Upstream exceeds 99th percentile	Number of 30-minute windows where upstream TB exceeded the site-specific 99th percentile threshold, based on pre-2018 background data.
	Downstream exceeds 99th percentile	Number of 30-minute windows where downstream TB exceeded the site-specific 99th percentile threshold, based on pre-2018 background data.

Statistical Analysis of Water Temperature and Turbidity

Water temperature and turbidity were analyzed by graphical inspection, descriptive statistics, analysis of magnitude and duration, and testing time-matched paired differences. At each site and for each period, bootstrapped resampling and confidence intervals were computed to test if the observed median of all time-matched paired differences between upstream and downstream were significantly different from zero. Water temperature and turbidity were each further analyzed by methods suited for each specific parameter in the following subsections.

The raw data were initially plotted over time for graphical inspection and used to calculate the minimum, first quartile (Q1), median, third quartile (Q3), and maximum for each site, station, and period.

An hourly median was computed to account for lag time between the downstream and upstream stations. The downstream hourly median data were plotted against the upstream data for visual inspection. The hourly median data were used to analyze magnitude and duration of the time-matched paired differences to identify potential short- and long-term anomalous conditions for both parameters. If there was not a complete concurrent pair, the difference was not calculated, and the given date time was removed from analysis. The hourly values were not calculated and removed from the analysis if there was less than 80-percent of the data in a given hour.

The instrument's uncertainty for water temperature is ± 0.15 °C, while turbidity measurements have an uncertainty of ± 0.3 FNU or 2-percent, whichever is greater (YSI, 2012). Differences calculations require accounting for the combined uncertainty from both the upstream and downstream instruments and were computed as averages for each site, station, and period as in JCGM (2020):

$$\frac{1}{n}\sum_{i=1}^{n}\sqrt{(x_{DSi})^2 + (x_{USi})^2} \quad (1)$$

where

n *is the number of observations*

i *is each instantaneous observation*

x_{DS}, x_{US} *are each downstream and upstream station observation, respectively*

A bootstrapping of median differences approach was used to determine if the difference between the hourly median time-matched paired observations between downstream and upstream stations differed significantly from zero. A non-parametric bootstrapping of medians approach is well-suited for large, non-normal, and asymmetric datasets (Johnston and Faulkner, 2021; Mudelsee and Alkio, 2007), which do not meet the assumptions of other statistical test for dependent samples. Additionally, Johnston and Faulkner (2021) found that the bootstrapping of differenced medians resulted in less Type I error in comparison to rank-banked Mann-Whitney Wilcoxon test, although the analysis tested two independent samples.

The bootstrapping of median differences test used in this analysis is a one-sample test applied to the dependent sample of time-matched paired differences between the upstream and downstream stations. The median of the observed distribution of differences is computed and used as the test statistic and compared to 10,000 bootstrapped resampled distributions with replacement. Recent studies have stressed that calculating p-values for classic null hypothesis statistical tests (NHST) when testing large sample sizes are not useful or appropriate because the tests are heavily influenced by and dependent on sample size (Lin and others, 2013; Krawczyk, 2015; Gómez-de-Mariscal and others, 2021). Alternatively, recent studies suggest evaluating

confidence intervals directly (Lin and others, 2013; Balkin and Lenz, 2021; Gómez-de-Mariscal and others, 2021). Upper and lower 99-percent confidence intervals were calculated for each station and period from 10,000 bootstrapped resampling, with replacement. The confidence intervals were evaluated for the hourly median differences of time-matched pairs between the downstream and upstream monitoring stations.

Results of the bootstrapping of median differences tests were evaluated as such:

> If a test's confidence interval overlaps zero, or the observed median of the time-matched paired differences is less than or equal to the combined uncertainty from instrument accuracy, then the observed median of the time-matched paired differences does not differ significantly from zero;

> If a test's confidence interval does not overlap zero and the observed median of the time-matched paired differences is greater than the combined uncertainty from instrument accuracy, then the observed median of the time-matched paired differences differs significantly from zero.

Bootstrapping of median differences tests were performed in R v4.4.2 (R Core Team, 2025). Bootstrapped resampling was completed using the base R function 'replicate.'

Continued Statistical Analysis of Water Temperature

The water temperature data were used to perform anomaly detection analysis on the hourly median differences between the upstream and the downstream gage sites. The duration and magnitude of the anomalies were calculated to assess potential short-term or long-term effects from pipeline stream crossing construction.

Water Temperature Anomaly Detection

Anomaly detection is used to determine significant or extreme measurements that differ significantly from the datasets overall distribution and are rare in the dataset (Jamshidi and others, 2022). Here, anomaly detection was used to elucidate changes from the hourly median water temperature differences at each paired pipeline crossing site. The hourly median water temperature measurement at the upstream site was subtracted from the concurrent downstream water temperature (downstream hourly median – upstream hourly median).

Anomalies were detected by decomposing the hourly median difference timeseries to eliminate the seasonality and the long-term, non-stationarity trend. The differenced time series (downstream – upstream) was decomposed using the Seasonal and trend decomposition using Locally Estimated Scatterplot Smoothing (LOESS) (STL), which separates the time series into three components: seasonal, trend, and the remainder (Shikwambana and Kganyago, 2023). The seasonal component represents the variation in the timeseries for a stated period, such as regular monthly intervals, to capture predictable patterns in the time series (Dancho and Vaughan, 2018; Shikwambana and Kganyago, 2023). The trend component reveals the long-term, low-frequency, non-stationary trends in the time series (Shikwambana and Kganyago, 2023). The remainder component represents the data remaining after removing the seasonal and the trend components

(Shikwambana and Kganyago, 2023). The STL method auto-calculated 24 days as the frequency and between 716 to 735 days for the trend across all sites. The frequency indicates the total number of days in a cycle within the dataset, and the trend is the period which can be aggregated to visualize the data's central tendency (Dancho and Vaughan, 2018).

Water temperature anomalies were detected using the generalized extreme studentized deviate (GESD) which uses a Student's t-test to remove outliers (Dancho and Vaughan, 2018). The test statistic is compared to a critical value; when an outlier is identified and removed, the test statistic is recalculated and updated (Dancho and Vaughan, 2018). All outliers are removed once the test statistic falls below the critical value (Dancho and Vaughan, 2018). A positive temperature anomaly indicates the downstream station is warmer than the upstream station and is referred to as a "downstream-warmer" temperature anomaly. A negative temperature anomaly indicates the upstream station is warmer than the downstream station as is referred to as an "upstream-warmer" temperature anomaly. The duration and the magnitude were calculated on each of the anomalies. The water temperature anomaly detection was performed in R-Studio R4.4.2 using the package "anomalize" (Dancho and Vaughan, 2023).

Continued Statistical Analysis of Turbidity

Turbidity and gage height data were used to conduct a hysteresis analysis of the storms at each site, station, and period. Storm hysteresis analyzes the temporal dynamics of peaks and troughs between a storm's hydrograph and a solute's chemograph (Liu and others, 2021; Lloyd and others, 2016a). This dynamic interplay between the hydrograph and chemograph are utilized to create hysteresis loops; for which, hysteresis metrics like, a hysteresis index can be computed to gain insights about biogeochemical and watershed processes, land use, anthropogenic changes, and hydroclimatic conditions (Knapp and others, 2020; Burns and others, 2019).

Stormflow Hysteresis

Hysteresis loops are characterized by their direction and magnitude (Lloyd and others, 2016a). Clockwise loops indicate rapid delivery with the peak of the chemograph on the rising limb of the hydrograph (Baker and Showers, 2019), while counter-clockwise loops indicate delayed delivery, with the peak of the chemograph on the falling limb of the hydrograph (Fovet and others, 2018).

A hysteresis index (HI) aids in the quantification of storm hysteresis by applying a consistent, representative metric to summarize a storm's hysteresis and was computed as (Lloyd and others, 2016a):

$$HI = T_{RL\_norm} - T_{FL\_norm} \qquad (2)$$

where

T_{RL_norm} is the normalized turbidity value on the rising limb of the hydrograph

$T_{FL_{norm}}$ is the normalized turbidity value on the falling limb of the hydrograph

Slopes indicate whether a storm event was enriching (chemograph graph was becoming more positive) or diluting (chemograph was becoming more negative). A "slope" metric is often evaluated (Waite and others, 2023; Musolff and others, 2021; Millar and others, 2022) along with HIs, which characterizes the hysteresis loop as positive, negative, or no slope (i.e., slope = 0). For this analysis, the slope was estimated as the line of best fit using an ordinary least squares linear regression between the natural logarithm of turbidity and natural logarithm of gage height. The sign of the numerical value of the slope indicates whether the dominant condition of a storm

event was enriching, diluting, or if neither was dominant. The relation between HI and slope is compared to better understand the types of hysteretic behaviors that occur when the concentration of the parameter of interest is enriching or diluting, providing insights and additional evidence about the proximity of sources and delivery dynamics.

High-frequency turbidity and gage height data were used to analyze hysteretic patterns at each site. Typically, discharge is used in hysteresis analysis instead of gage height; however, discharge data were not collected at most stations. Only the Roanoke River gage 02054500 had both gage height and discharge data available. A preliminary hysteresis analysis was performed for the upstream and downstream stations of the Roanoke River using both gage height and discharge, and results showed agreement.

Hysteresis analysis was performed on all storm events where gage height and turbidity data at both upstream and downstream stations were available and contained 10-percent or less gaps in turbidity data. Prior to analysis, time series gaps were filled by linear interpolation. Each individual storm's hysteresis loop, hydrograph, and chemograph were inspected to evaluate if interpolated data resulting from data gaps affected the hysteresis index value. Any storm hysteresis loop where interpolated data changed the prevailing shape and magnitude of the loop was removed from further analysis.

All analyses were performed in R v4.4.2 (R Core Team, 2025). Baseflow separation, storm identification, peak identification, and rising and falling limb parsing was completed using the "hydroEvents" package (Wasko and Guo, 2022).

Short- and Long-term Water Temperature Patterns

Quantifying the duration and magnitude of temperature anomalies in streams before, during, and after pipeline crossing construction is pertinent to contextualizing the potential impacts construction may cause on the aquatic ecosystem and water quality. Short-duration thermal fluctuations can significantly stress aquatic species, potentially resulting in sublethal impairments or mortality events under extreme conditions (Alfonso and others, 2021; Donaldson and others, 2008; Johnson and others, 2024, Tassone and others, 2023). Longer-duration warming temperatures could result in a variety of ecological consequences, such as a change to the physiology, behavior, and phenology in individual species, the migration of biota to new habitat, and potential trophic restructuring (Johnson and others, 2024). The toxicity of pollutants such as ammonia, pesticides, and polyaromatic hydrocarbons may also increase with increasing temperature (Berger and others, 2017; Erickson, 1985; Noyes and Lema, 2015; Verheyen and others, 2022). Here, the magnitude and duration of water temperature anomalies were investigated to assess the potential for short-term and long-term effects from the pipeline crossing construction on the overall thermal regime.

Comparative Analysis of Upstream and Downstream Water Temperature Conditions

The upstream and downstream temperatures have a similar seasonal variation throughout the study period, following the typical U.S. East Coast seasonal temperature regimes (Figure 3A). Across all paired sites, the hourly median temperatures ranged from -2 to 30.4 °C (Table 4). January consistently had the coldest median temperatures at both the upstream and downstream sites throughout the study. The warmest median temperatures occurred during July for all sites, except for upper Bottom Creek, where peak median temperatures were recorded in August.

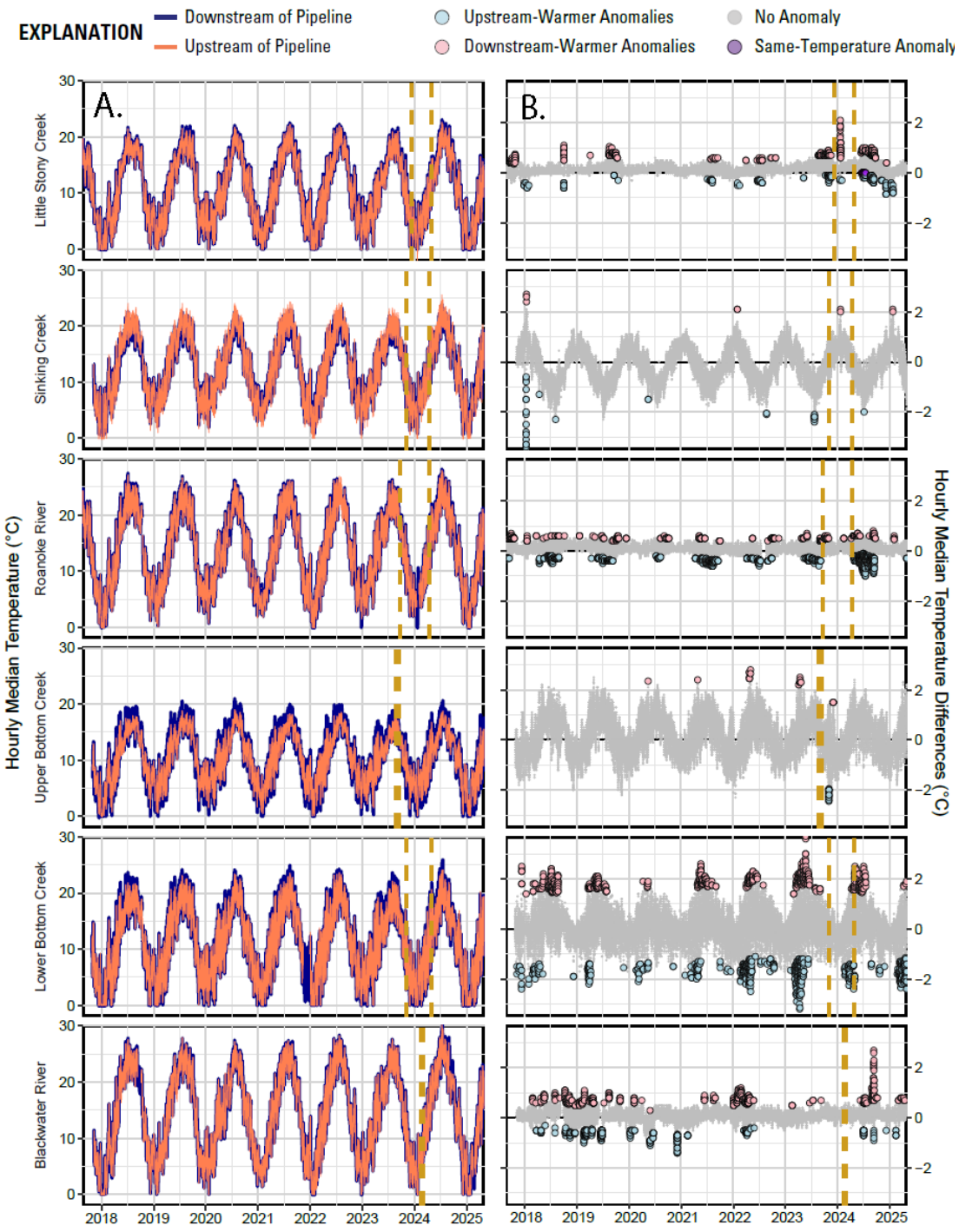

Figure 3. Time series of the hourly median water temperature. Vertical dashed lines indicate the during crossing construction period. *A,* Time series of the upstream and downstream sites for each paired station, *B,* Time series of the downstream – upstream and the identified temperature anomalies when seasonality and long-term trends were removed.

The hourly median water temperature differences between the upstream and downstream stations were used to visually observe thermal variations on both an interannual and seasonal timescale for each of the six sites (Figure 3B). A negative hourly median temperature difference indicates the upstream station had a higher hourly median temperature than the downstream station. A positive hourly median temperature difference indicates that the downstream station had a higher hourly median temperature than the upstream station.

Sinking Creek, upper Bottom Creek, and lower Bottom Creek demonstrated the most pronounced seasonal variation throughout the monitoring period. However, upper and lower Bottom Creek exhibited a different pattern than Sinking Creek. At the Bottom Creek sites, the downstream station's hourly median temperature had warmer temperatures than the upstream station during the warmer, summer months (Figure 3B). In contrast, the upstream station had higher hourly median temperatures than the downstream station in the warmer, summer months (Figure 3B). Little Stony Creek, Roanoke River, and Blackwater River had less variation seasonally and interannually in the hourly median temperature differences between upstream and downstream.

To further explore these patterns, temperature differences were evaluated at all sites by isolating the before, during, and after stream crossing construction periods. Within each site and each period, the upstream and downstream station generally had similar temperatures (Figure 4, Table 4), although there were site-specific differences. At Sinking Creek, there were higher temperatures at the upstream station compared to the downstream station at warmer overall temperatures in the before and after periods (Figure 4B). Upper and lower Bottom Creek showed warmer downstream temperatures as the temperature increased during all three periods (Figure 4D, Figure 4E). In the during construction period, upper Bottom Creek notably diverged from

the 1-to-1 line (that is, the line where downstream temperature equivalent is to upstream temperature) (Figure 4D), with a higher temperature at the downstream station compared to the upstream station.

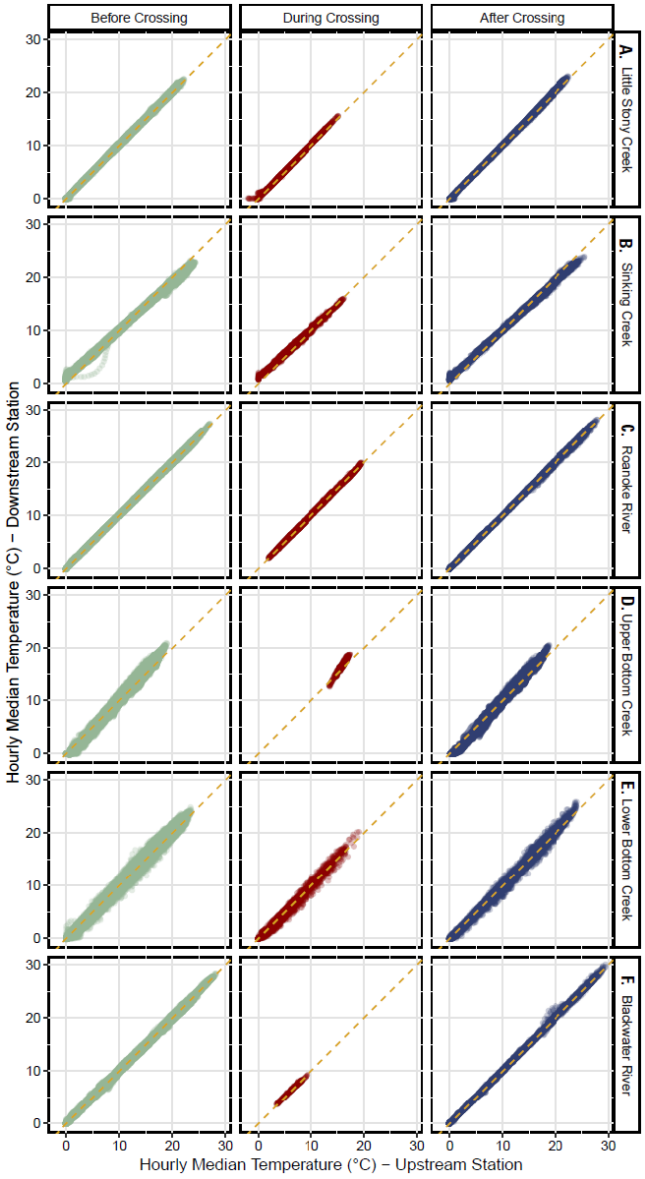

Figure 4. Scatterplot of each paired station in the before, during, and after period. The 1-to-1 golden dashed line represents when the upstream and downstream hourly median temperatures are equivalent. *A,* Little Stony Creek; *B,* Sinking Creek; *C,* Roanoke River; *D,* upper Bottom Creek, *E,* lower Bottom Creek, *F,* Blackwater River.

Table 4. Characterization of the distribution of the high-frequency (5-minute interval) data of water temperature at all sites throughout the before crossing, during crossing, and after crossing construction.

[°C, degrees Celsius; N, Sample Size; Min, Minimum; Q1, Quantile 1; Q3, Quantile 3; Max, Maximum]

		Upstream						Downstream					
			°C						°C				
Location	Period	N	Min	Q1	Median	Q3	Max	N	Min	Q1	Median	Q3	Max
Little Stony Creek	Before	655,221	-0.1	5.7	10.7	16.3	22.2	628,727	-0.1	5.8	10.8	16.4	22.6
	During	40,248	-2	3.5	5.3	8	15.3	40,229	0	3.7	5.6	8.2	15.7
	After	105,604	-0.1	5.6	12	16.5	22.6	104,303	-0.1	5.8	12.3	16.7	23.1
Sinking Creek	Before	619,843	-0.2	7.6	12.8	18.4	24.3	621,368	0.4	8	12.6	17.6	23.2
	During	47,429	-0.1	5.2	7.1	9.6	16.3	47,420	0.7	5.9	7.6	9.9	16.2
	After	106,305	-0.1	8.1	14.5	18.4	25.6	108,934	0.5	8.2	14	17.7	23.9
Roanoke River	Before	615,825	-0.1	7.7	14	20.1	27.1	620,495	-0.1	7.8	13.7	19.9	27.5
	During	54,409	1.9	6.2	9	12.6	19.6	59,124	-0.1	6	8.7	12.4	20
	After	108,613	-0.1	8	15.4	19.9	27.9	109,518	-0.1	8.1	15.6	20.1	28.3
Upper Bottom Creek	Before	600,063	-0.1	6.7	10.3	14.3	19	601,436	-0.3	6.3	10.4	15	21
	During	5,746	13.5	15.4	15.9	16.3	17.4	5,761	12.6	15.8	16.5	17	18.8
	After	170,845	0.1	6	9.1	13.1	18.8	166,058	-0.1	5.4	8.9	13.3	20.7
Lower Bottom Creek	Before	631,013	0	6.2	11.5	16.7	23.7	617,947	-0.2	6.1	11.6	17	24.9
	During	50,661	0	3.9	6.1	8.9	19.1	50,649	-0.1	3.7	5.9	8.8	20.4
	After	105,474	-0.1	6.2	12.7	16.4	24.1	106,471	-0.2	6.1	12.7	16.6	26
Blackwater River	Before	632,181	-0.1	7.2	13.9	21	28.3	636,464	-0.1	7.2	13.9	21.1	28.4
	During	2,904	3.3	5.2	6.6	7.6	9.3	2,903	3.6	5.4	6.8	7.7	9.3
	After	107,094	-0.2	8.8	14.7	20.7	30.2	109,034	-0.1	8.3	14.7	20.9	30.4

The finding that, in general, the upstream and downstream hourly water temperature differences were similar was supported by the bootstrapping of median differences analysis of the hourly median differences (Table 5). The observed median differences ranged from the upstream warmer by 0.15 °C and the downstream warmer by 0.6 °C. Sixteen of the 18 tests had hourly median differences less than the combined uncertainty from the instrumentation. Of these, three tests also had confidence intervals that overlapped zero – lower Bottom Creek in the before and after period and upper Bottom Creek in the after period. Sinking Creek and upper Bottom Creek in the during period are the only two tests which may have significant results because the

observed median of differences is greater than the combined instruments uncertainty and the confidence intervals do not overlap zero. For these two tests that yielded a significant result, the maximum median of differences is less than 1°C when uncertainty is accounted for, ranging from 0.24 to 0.66 °C at Sinking Creek and from 0.39 to 0.81 °C at Upper Bottom Creek in the during period.

Table 5. Results of the bootstrapped hourly median differences between the upstream and downstream time-matched paired water temperature differences the before, during, and after crossing period. A negative median temperature, lower 99-percent confidence interval, and upper 99-percent confidence interval indicates that the upstream site was warmer than the downstream site and a positive temperature value indicates that the downstream site was warmer than the upstream.

[°C, degrees Celsius; N, Sample Size; CI, confidence interval; %, percent]

Location	Period	N	°C				
			Combined uncertainty from instruments	Median of hourly median differences	Lower 99% CI	Upper 99% CI	Range between upper and lower 99% CI
Little Stony Creek	Before	54,253	±0.21	0.1	0.1	0.1	0
	During	3,379	±0.21	0.2	0.2	0.2	0
	After	8,683	±0.21	0.15	0.15	0.2	0.05
Sinking Creek	Before	51,981	±0.21	-0.1	-0.1	-0.1	0
	During	3,975	±0.21	0.45	0.45	0.5	0.05
	After	8,837	±0.21	-0.15	-0.2	-0.1	0.1
Roanoke River	Before	50,476	±0.21	0.1	0.1	0.1	0
	During	4,541	±0.21	0.1	0.1	0.1	0
	After	9,047	±0.21	0.1	0.1	0.1	0
Upper Bottom Creek	Before	50,192	±0.21	0.2	0.2	0.2	0
	During	501	±0.21	0.6	0.5	0.6	0.1
	After	13,798	±0.21	0	-0.1	0	0.1
Lower Bottom Creek	Before	52,079	±0.21	0	0	0	0
	During	4,245	±0.21	-0.1	-0.1	-0.1	0
	After	8,786	±0.21	0	0	0	0
Blackwater River	Before	52,742	±0.21	0.1	0.1	0.1	0
	During	286	±0.21	0.2	0.1	0.2	0.1
	After	9,336	±0.21	0.1	0.1	0.1	0

Detection of Water Temperature Anomalies

Across the six sites, 7,284 hourly median water temperature anomalies were detected out of the 766,504 total hourly median differences, representing approximately 0.95-percent of the data. Roanoke River, lower Bottom Creek, and Blackwater River had the highest percentage of data that detected anomalies, at 1.72-percent (n = 2,171 of 126,450), 1.55-percent (n = 2,010 of 129322), and 1.45-percent of the data (n = 1,794 of 123682), respectively. Anomalies were detected at Little Stony Creek in 0.89-percent of the data (n = 1,152 of 129,656). There were two sites with less than 100 anomalies detected in the time series and consisting around 0.06-percent of the data – at Sinking Creek (n = 80 of 128,984) and upper Bottom Creek (n = 76 of 128,410).

There were three types of anomalies detected: downstream-warmer, which accounted for 3,218 anomalies (44.2-percent), upstream-warmer, which accounted for 4,030 anomalies (55.3-percent), and same-temperature anomalies, which accounted for 36 total anomalies (0.9-percent). Throughout the study period, the median duration of all anomaly types was two hours and the median temperature difference of 0.73 °C, in which the downstream station is warmer. This report further investigates the magnitude and duration of downstream-warmer and upstream-warmer anomalies.

Downstream-Warmer Anomalies

Downstream warmer anomalies accounted for 47-percent of all anomalies in the before period (n = 1,219), 60-percent in the during period (n = 68), and 34-percent in the after period (n = 322). The highest number of downstream-warmer anomalies occurred in the before period, comprising 76-percent of all downstream-warmer anomalies (n = 1,219 pf 1,609), likely due to the longer duration of the period. There were 68 and 322 total downstream-warmer anomalies in

the during and after period, respectively. There were downstream-warmer anomalies in the during construction period at Little Stony Creek, Sinking Creek, the Roanoke River, and lower Bottom Creek.

Downstream-warmer anomalies varied in their median magnitude for a given event between 0.3 to 3.0 °C (Figure 5). The highest temperature difference occurred at lower Bottom Creek in the before period, in which the downstream site was 3.0 °C higher than the upstream site and lasted for six hours. The downstream-warmer anomalies had a duration less than a day, ranging from 1 to 18 hours. Two of the longest duration events, both lasting 18 hours, occurred at Little Stony Creek; one in the before period with a median temperature difference of 0.60 ± 0.21 °C and the second in the during period with a median temperature difference of 0.90 ± 0.21 °C.

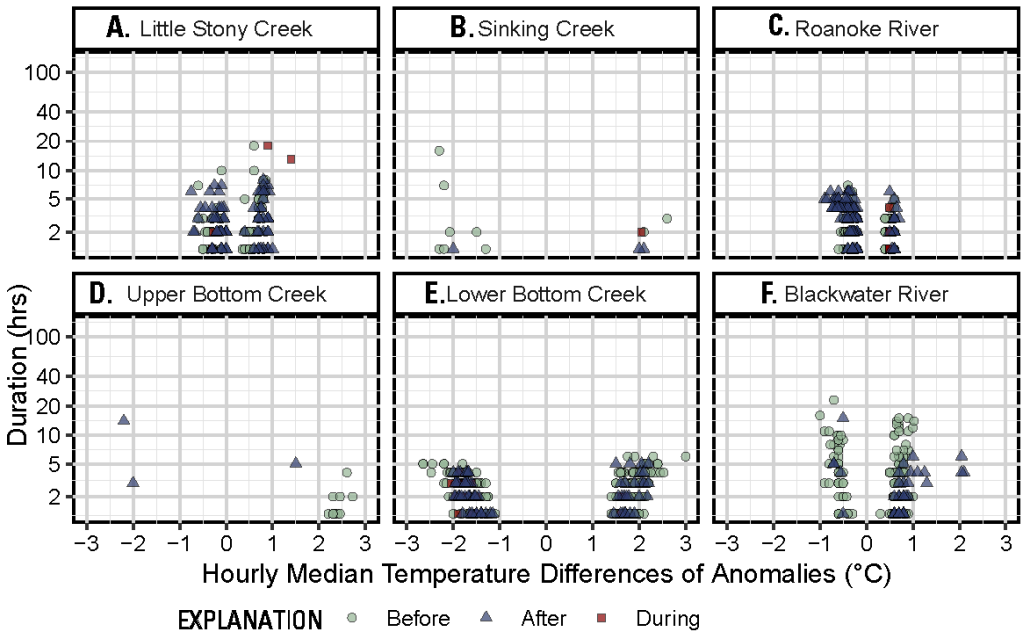

Figure 5. Scatterplot of the hourly median temperature difference of the anomalies and the duration, in hours, of the anomalies in the before, during, and after period. *A,* Little Stony Creek; *B,* Sinking Creek; *C,* Roanoke River; *D,* Upper Bottom Creek, *E,* Lower Bottom Creek, *F,* Blackwater River.

Upstream-Warmer Anomalies

Most upstream-warmer anomalies were detected in the before period (n = 1,356 of the 2,575 or 52-percent), likely due to longer duration of the period. In the during period, there were 46 anomalies detected out of the 114 total anomalies detected in the during period, representing 40-percent. In the after period, upstream-warmer anomalies represent 613 of the total 953 anomalies in the after period, or 64-percent. There were upstream-warmer anomalies identified only at Little Stony Creek and Lower Bottom Creek in the during crossing construction period. The upstream-anomalies were most prevalent at Sinking Creek (n = 62 of 80 anomalies, or 78-percent) followed by the Roanoke River (n = 1,626 of 2,172, or 75-percent) and lower Bottom Creek (n = 1,020 of 2,010, or 51-percent).

During the study period, the median duration of all anomaly types was 2 hours and the median temperature difference of 0.42 °C, in which the upstream station was warmer. The upstream-warmer anomalies varied in their magnitude between 0.050 to 2.65 °C (Figure 5). The highest temperature difference occurred at lower Bottom Creek in the before period, in which the upstream site was 2.65 °C higher than the downstream site and persisted for 5 hours. The longest-lasting upstream-warmer temperature anomaly persisted at Blackwater River for 134 hours, with a median temperature magnitude of 0.60 ± 0.21 °C.

Discussion of Water Temperature Results

At all monitored locations, the upstream and downstream site exhibited a similar thermal behavior within each evaluated period. The differences between the paired sites were minimal, with the range between the lower and upper 99-percent confidence intervals from 0 to 0.1 °C. Twelve of 18 tests had a difference in the upper and lower 99-percent confidence intervals of 0

°C. The median of the hourly median differences was also small, between -0.15 to 0.6 °C for all sites and periods. Of the 18 tests performed, only Sinking Creek in the during period and upper Bottom Creek in the during period were statistically significant. At both sites in the during period, the medians of hourly median differences exceeded the combined uncertainty of the instrumentation, and the confidence interval did not include 0. Although these tests are statistically significant, the range of the temperature differences at both sites is less than 1 °C, with Sinking Creek at 0.24 – 0.66 °C and upper Bottom Creek from 0.39 – 0.81 °C.

To distinguish any potential differences between the upstream and downstream temperatures, water temperature anomaly detection was utilized to remove the effects of seasonality and long-term changes to detect potential anomalous events. There were both downstream-warmer and upstream-warmer anomalies across all study sites; however, these anomalies constituted approximated 1-percent of the total data collected. Most of the downstream-warmer and upstream-warmer anomalies were identified in the before period due to the length of the before period in comparison to the during and after. Sites that used the trenchless construction crossing method detected downstream-warmer anomalies in the during period, whereas the two sites using trenched crossing methods did not detect any anomalies; however, this disparity is more closely linked to the duration of the crossing period than the crossing technique itself. The trenched construction period lasted 12 days at Blackwater River and 21 days at Upper Bottom Creek, while the trenchless crossing period had a duration between 141 to 208 days. Additionally, some of the sites displayed a notable seasonality that was captured in the during period. For instance, at lower Bottom Creek and the Roanoke River, there are downstream-warmer anomalies in the late-spring to early-summer months and upstream-warmer anomalies.

Both the duration and magnitude of the downstream-warmer and upstream-warmer anomalies were relatively short duration and low magnitudes. The median duration across all anomaly types was 2 hours, with a median magnitude of 0.73 ± 0.21 °C, with the downstream at a higher temperature than the upstream. Little Stony Creek, Roanoke River, lower Bottom Creek, and Blackwater River displayed comparable ranges for upstream- and downstream-warmer anomalies and demonstrate a consistent pattern across different periods. The duration and magnitudes of the anomalies in the during crossing construction period aligned closely to those of the before and after crossing construction period.

The median duration of both upstream-warmer and downstream-warmer were both 2 hours, indicating that in general, anomalies were not persisting over long durations in the streams. The maximum duration of a downstream-warmer anomaly was less than 1 day, at 18 hours, and the duration of an upstream-warmer anomaly was 134 hours. While there are longer duration anomalies, 61-percent of the upstream-warmer anomalies (n = 380 of 610) and downstream-warmer anomalies (n = 441 of 722) are less than or equal to 2 hours in total duration. About 90-percent of the data has a duration less than or equal to 4 hours, with 649 of 722 upstream-warmer anomalies (90-percent) and 539 of 610 downstream-warmer anomalies (88-percent), suggesting that most of the anomalies are short in duration.

The median magnitude of the downstream-warmer anomalies was 0.74 °C, and the median magnitude of the upstream-warmer anomalies was 0.43 °C. Some sites had a consistent typical range in the upstream-warmer and downstream-warmer anomalies, such as Little Stony Creek, lower Bottom Creek, and the Roanoke River (Figure 5). All the sites had similar magnitudes of temperatures consistent throughout the before, during, and after period. Most of these magnitudes between the upstream and downstream sites are small, with about 63-percent of

the downstream-warmer anomalies (n = 385 of 610) and 68-percent (n = 493 of 722) of the upstream-warmer anomalies less than or equal to 1°C. 90-percent of the downstream-warmer anomalies are less than or equal to 2 °C difference between upstream and downstream and an even higher percentage, 97-percent (n = 702 of 722) of the upstream-warmer anomalies. Over the 7-year study period, the magnitude of the temperature anomalies was low; most detected anomalies were within a 2 °C difference.

One criterion applied in the real-time alert application included flagging instances where the temperature differences between upstream and downstream exceeded the natural temperature variability threshold, defined as 1-3 °C depending on the stream class (Virginia Administrative Code 9VAC25-260-50). None of the study sites recorded hourly temperature differences exceeding 3 °C, indicating that the temperature anomalies generally remained within the expected range for Virginia. There was only one temperature anomaly difference which had a median temperature difference of exactly 3 °C. This occurred during the before period at lower Bottom Creek from 05/23/2029 at 12:00 to 05/23/2017 at 17:00. However, the small number of hourly median temperature anomalies with respect to the entire dataset, combined with the brief duration and low magnitude of anomaly events, suggests that the crossing construction on the pipeline had minimal impact on the thermal regime downstream.

The anomaly detection method used in the analysis removes the effect of long-term trends in the water temperature but does not remove the effect of short-term changes in temperatures. Temperature is a highly variable metric that is significantly influenced by air temperature and environmental conditions, including channel geometry, water depth, tributary confluences, groundwater seeps, stream discharge levels, and microhabitat characteristics (Caissie, 2006; Siegel and Volk, 2019; Gendaszek and Appel, 2022; Mejia and others, 2020).

While air temperature was not directly measured in this study, stream water temperature increases about 0.6 to 0.8 °C for every 1 °C increase in air temperature (Morrill and others, 2005). However, higher elevations or groundwater-dependent watersheds are less sensitive to temperature changes (Siegel and Volk, 2019). For example, from direct field observation, Sinking Creek has a groundwater input located downstream of the upstream monitoring location amongst other known groundwater inputs within the watershed (Christensen and others, 2022). The groundwater discharge cools the surface water in the summer (Gendaszek and Appel, 2022) and results in the more upstream-warmer temperature anomalies, and the upstream site was warmer in the summer months (Figure 3). The confluence of tributaries could potentially influence temperature differences at the upstream or downstream site. At the Blackwater River, there are two confluences from tributaries near the Blackwater River upstream site (Figure 2F) which could potentially influence conditions observed at the upstream or downstream location. The confluence upstream of the Blackwater River upstream site, Maggodee Creek, was also crossed by the MVP. Maggodee Creek, which has a watershed area of 45.5 mi^2 (U.S. Geological Survey, 2019) was crossed using trenched methods and overlapped the construction on the Blackwater River for 10 days.

Short- and Long- Term Patterns of Turbidity

Increased turbidity might degrade water quality, adversely affect lotic food webs, and disrupt ecosystem function. Short-duration increases in turbidity have been associated with decreased primary production, zooplankton, benthic habitat diversity, hyporheic exchange, invertebrate abundance, and local fish populations (Henley and others, 2000; Huenemann and others, 2012; Honious and others, 2022). Longer-duration turbidity increases have been shown to

exacerbate and prolong the potential effects that have been associated with short-term turbidity increases (Henley and others, 2000). Here, the magnitude and duration of potential anomalous turbidity conditions from pipeline crossing construction were investigated and compared to each stream's turbidity regime.

Turbidity Conditions and Comparison of Upstream versus Downstream Stations

Upstream median turbidity ranged from 0.5 to 7.2 FNU across all sites and periods, and the downstream ranged from 0.6 to 8.3 FNU (Table 6). Higher turbidity at both upstream downstream stations was typically associated with increased gage height throughout the study period and lower turbidity at low gage height, as expected (Figure 6; Appendix 1.1-1.3). The Blackwater River had the highest magnitude turbidity values across all summary statistics and upper Bottom Creek had the lowest (Table 5). At all sites and during all periods, the minimum, Q1, median, and Q3 are close together in magnitude compared to their maximums.

Little Stony Creek, Roanoke River, upper Bottom Creek, and Blackwater River displayed general agreement in the time series data over the entire study period. Sinking Creek turbidity peaks during storms were consistently higher at the upstream stations before the stream crossing and in the during and after crossing periods were closer together. Lower Bottom Creek had consistently higher turbidity at the downstream station compared to the upstream station over the entire study period and anomalously high magnitude turbidity at the downstream station when compared to the upstream station in the during crossing period.

Table 6. Descriptive statistics of turbidity (in Formazin Nephelometric Units, FNU) for each site, station and period. Statistics were calculated using the raw 5-minute interval data and include N, number of observations; Min, minimum value; Q1, first quartile; Median, median value; Q3, third quartile; and Max, maximum value.

		Upstream						Downstream					
			FNU						FNU				
Location	Period	N	Min	Q1	Median	Q3	Max	N	Min	Q1	Median	Q3	Max
Little Stony Creek	Before	628,825	0	0.5	1.1	2	1,000	601,571	0	0.7	1.2	2.1	995
	During	35,856	0	0.9	1.3	2.1	237	31,192	0.9	1.5	1.9	2.4	281
	After	97,178	0	0.5	0.8	1.4	404	92,918	0	0.1	0.9	1.8	641
Sinking Creek	Before	564,619	0	1.5	3.3	6	1,000	579,228	0	1.9	3.8	6.6	913
	During	45,675	0	0.5	1.7	3.6	496	45,598	0	1	2	3.7	508
	After	87,419	0	0.8	2	4.1	945	102,598	0	0.9	2.9	5.7	1,000
Roanoke River	Before	590,320	0	1	2.1	4.6	1,000	589,319	0	1.1	2.2	4.6	1,000
	During	53,900	0	0.9	1.4	2.5	620	58,135	0.2	1	1.5	2.6	562
	After	105,034	0	0.6	1.8	4.6	897	102,500	0	0.8	1.8	4.6	847
Upper Bottom Creek	Before	581,135	0	0.2	0.6	1.1	783	588,343	0	0.2	0.6	1.2	700
	During	5,969	0.1	0.9	1.2	1.6	120	5,970	1	1.8	2	2.4	64.5
	After	142,844	0	0.1	0.5	1.3	321	157,568	0	0.2	0.8	2	325
Lower Bottom Creek	Before	614,258	0	0.7	1.3	2.2	1,000	578,988	0	2	2.9	4.7	945
	During	45,716	0	0.5	0.9	2.2	111	48,422	0	1.8	3.1	6.1	797
	After	94,690	0	0.6	1.3	2.8	735	100,170	0.3	1.2	2.1	3.4	789
Blackwater River	Before	586,968	0	4.4	7.2	14.2	1,000	577,120	0.2	4.1	7.1	14.9	1,000
	During	3,144	3.7	4.7	5.6	9.9	178	3,131	3.1	5.9	8.3	12.4	224
	After	100,410	0.5	2.6	4.4	8.1	978	86,273	0	2.8	4.8	10.6	1,000

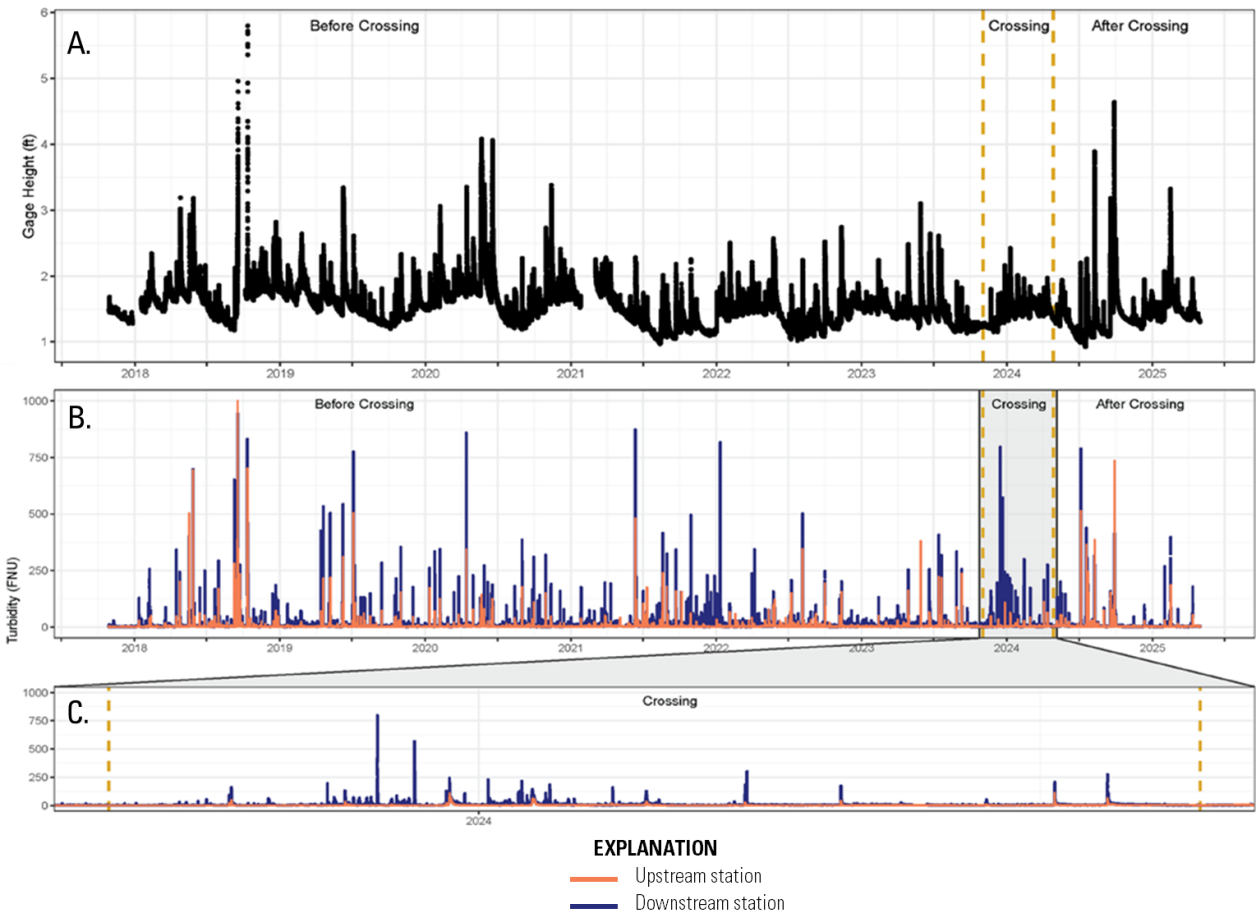

Figure 6. High-frequency turbidity and gage height time series at Lower Bottom Creek in the before crossing, during crossing, and after crossing periods. *A,* Gage Height at Downstream Lower Bottom Creek (0205373422); *B,* Turbidity at the Upstream (0205373228) and downstream (0205373422) Lower Bottom Creek; *C,* Turbidity in the during crossing period. Refer to Table 1 for additional information about USGS sites.

Differences between downstream and upstream stations of the hourly median turbidity values show anomalous behavior in the during crossing period at lower Bottom Creek shown by the red points ascending the y-axis without a matching signal of the same magnitude on the x-axis (Figure 7). Most observations at lower Bottom Creek during the crossing appear to be left of the 1-to-1 line, suggesting many more observations where the downstream station had a higher

magnitude than the upstream station. The Blackwater River has a similar signal with downstream turbidity exceeding upstream turbidity in the during crossing period as did the Roanoke River in the after crossing period. The other sites and periods generally are close to the 1-to-1 line or are evenly distributed about it.

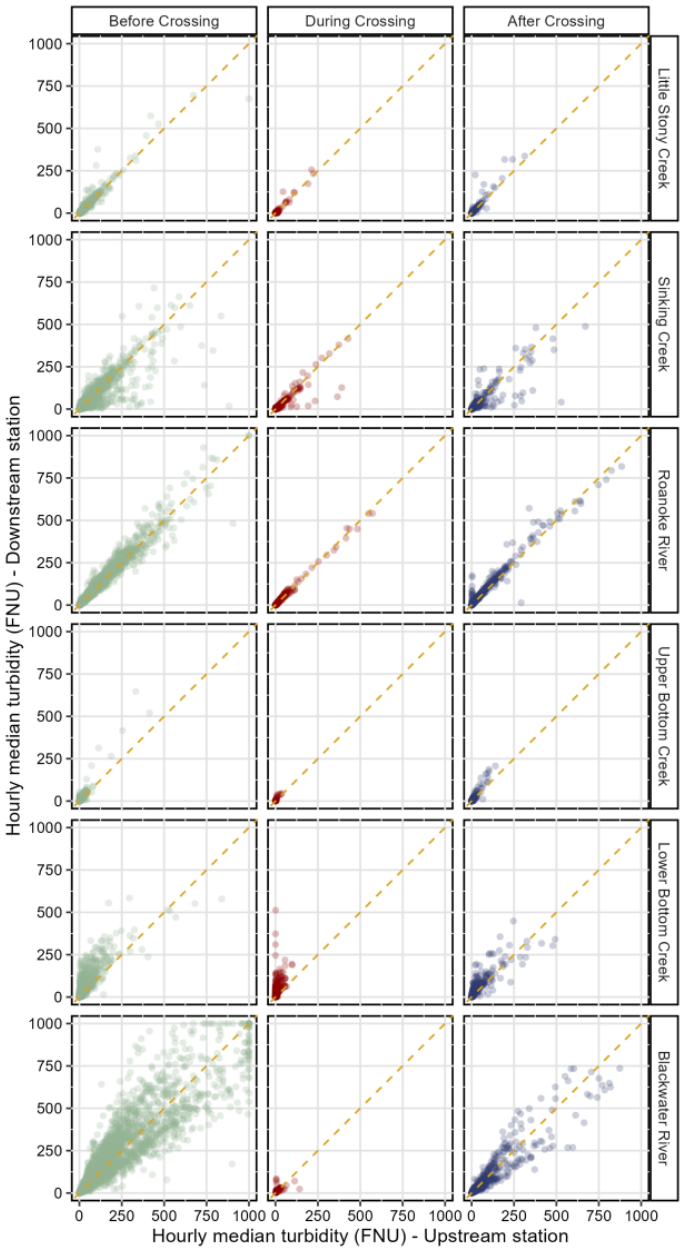

Figure 7. Hourly median turbidity at downstream station versus upstream station in the before, during, and after period. The golden dashed line is a 1-to-1 line.

Of the 18 comparisons (six matched sites * three periods), 15 had time matched differences of less than or equal to 5 FNU during 90-percent of the time series. The remaining three comparisons had differences less than or equal to 5 FNU for 80-to-89-percent of the time series (Appendix Table 1.2). Differences between upstream and downstream stations that were greater than 100 FNU represented less than or equal to 0 to 0.8 percent of the time series across all matched sites (Appendix Table 1.2).

Distributions of median hourly turbidity differences between stations show most of the observations are close to zero at all sites and all periods (Figure 8). At Sinking Creek, the largest magnitude differences occurred in the before crossing period with more total observations where the upstream station had higher turbidity than the downstream station. The Roanoke River had some larger magnitude differences in the after crossing period where the downstream station measurements were higher than the upstream station that was attributable to the presence of the pipeline ROW. At upper Bottom Creek, there were a small number of observations with larger differences in the before crossing period where the downstream station measured higher than the upstream station, and in the after crossing period a small number of larger differences where the upstream station measured higher than the downstream station. At lower Bottom Creek, the before and during crossing periods both showed a consistent signal of the downstream station measuring higher turbidity than the upstream station, with slightly more observations and greater magnitude observations occurring in the during crossing period. Most differences at lower Bottom Creek were still close to zero. At Blackwater River, all periods showed most differences close to zero, and a more normal distribution of values with roughly even amounts of observations greater than and less than zero. At Little Stony Creek, most differences for all periods were close to zero.

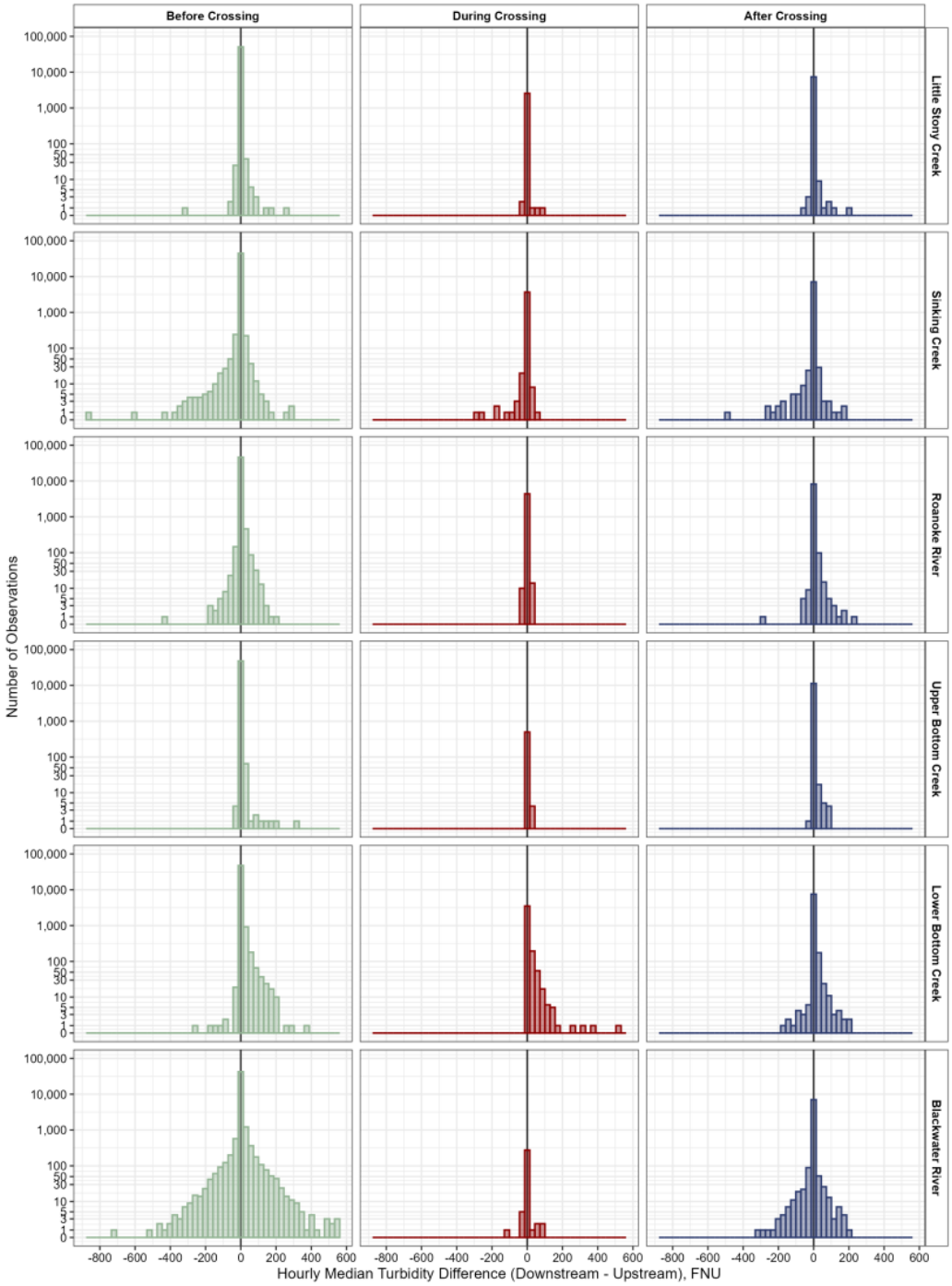

Figure 8. Histograms showing the baseflow turbidity differences between the upstream and the downstream site in the before, during, and after crossing period compared to the frequency of observations. A positive turbidity indicates the downstream turbidity was higher and a negative turbidity indicates the upstream turbidity was higher.

The bootstrapped median differences confidence intervals tests resulted in 3 of the 18 tests confidence intervals overlapped zero, suggesting strong evidence that the median does not differ significantly from zero. Nine additional tests (12 total tests) resulted in observed medians of the time-match paired differences lower than the amount of uncertainty from instrument accuracy, suggesting that these tests did not differ significantly from zero (Table 7). The six remaining tests overcame uncertainty from instrument accuracy and had confidence intervals that did not overlap zero, included Little Stony Creek during crossing, upper Bottom Creek during crossing, lower Bottom Creek before during and after crossing, and Blackwater River during crossing, suggesting that the median of the time-matched paired differences differed significantly from zero for these tests. When the uncertainty from instrument accuracy is accounted for in the six tests that yielded a significant difference, only two tests had a median of the differences that was reliably over 1 FNU, the before and during crossing periods at lower Bottom Creek which ranged from 1.19 to 2.11 FNU and 1.42 to 2.38 FNU, respectively. These two tests at lower Bottom Creek represent the largest magnitude upstream-to-downstream differences but are small in any practical meaning, were present in the before crossing period, and had the smallest observed median of upstream-to-downstream differences in the after crossing period.

Table 7. Results of the bootstrapped median of hourly median differences between the upstream and downstream time-matched paired turbidity observation in the before, during, and after crossing period.

[FNU, Formazin nephelometric unit; N, sample size; %, percent; CI, confidence interval]

Location	Period	N	FNU				
			Combined uncertainty from instruments	Median of hourly median differences	Lower 99% CI	Upper 99% CI	Range between upper and lower 99% CI
Little Stony Creek	Before	50,713	±0.44	0.2	0.2	0.2	0
	During	2,571	±0.44	0.7	0.7	0.75	0.05
	After	7,419	±0.44	-0.1	-0.1	0	0.1
Sinking Creek	Before	45,402	±0.51	0.3	0.3	0.35	0.05
	During	3,705	±0.48	0.25	0.2	0.3	0.1
	After	7,189	±0.48	0.3	0.3	0.35	0.05
Roanoke River	Before	46,785	±0.57	0.1	0.1	0.1	0
	During	4,405	±0.48	0.05	0	0.1	0.1
	After	8,321	±0.56	0.3	0.3	0.3	0
Upper Bottom Creek	Before	48,057	±0.43	0.05	0.05	0.1	0.05
	During	501	±0.43	0.9	0.85	1	0.15
	After	11,350	±0.43	0.4	0.4	0.4	0
Lower Bottom Creek	Before	48,918	±0.46	1.65	1.6	1.65	0.05
	During	3,804	±0.48	1.9	1.8	2.05	0.25
	After	7,789	±0.48	0.85	0.8	0.9	0.1
Blackwater River	Before	45,624	±0.90	0.25	0.25	0.3	0.05
	During	286	±0.49	1.3	1.15	1.5	0.35
	After	7,323	±0.64	-0.1	-0.1	0	0.1

Storm Hysteresis Patterns of Turbidity

At all stations and for all periods, the median hysteresis index (HI) and median slope were both positive, indicating turbidity tend to increase during storm events compared to ambient conditions and peaked on the rising limb of the hydrograph (Figure 9). A similar pattern was observed for all individual storm events at each station and across all periods, which is consistent with other stream turbidity hysteresis studies (Figure 1.4; Lloyd and others 2016b; Waite and others, 2023). Over the entire study period and at both upstream and downstream stations, positive HI was observed 182 times at Little Stony Creek, 137 times at Sinking Creek, 59 times

at Roanoke River, 98 times at upper Bottom Creek, 193 times at lower Bottom Creek, and 109 times at Blackwater River. Negative HI was observed 2 times at Little Stony Creek, 18 times at Sinking Creek, 37 times at Roanoke River, 0 times at upper Bottom Creek, 2 times at Lower Bottom Creek, and 36 times at Blackwater River; however, many HI values were close to zero, indicating no hysteresis. A threshold of -0.05 to 0.05 HI was used following Waite and others (2023) as a threshold to demonstrate hysteresis or not. No hysteresis was observed 12 times at Little Stony Creek, 25 times at Sinking Creek, 27 times at Roanoke River, 2 times at upper Bottom Creek, 13 times at lower Bottom Creek, and 47 times at Blackwater River.

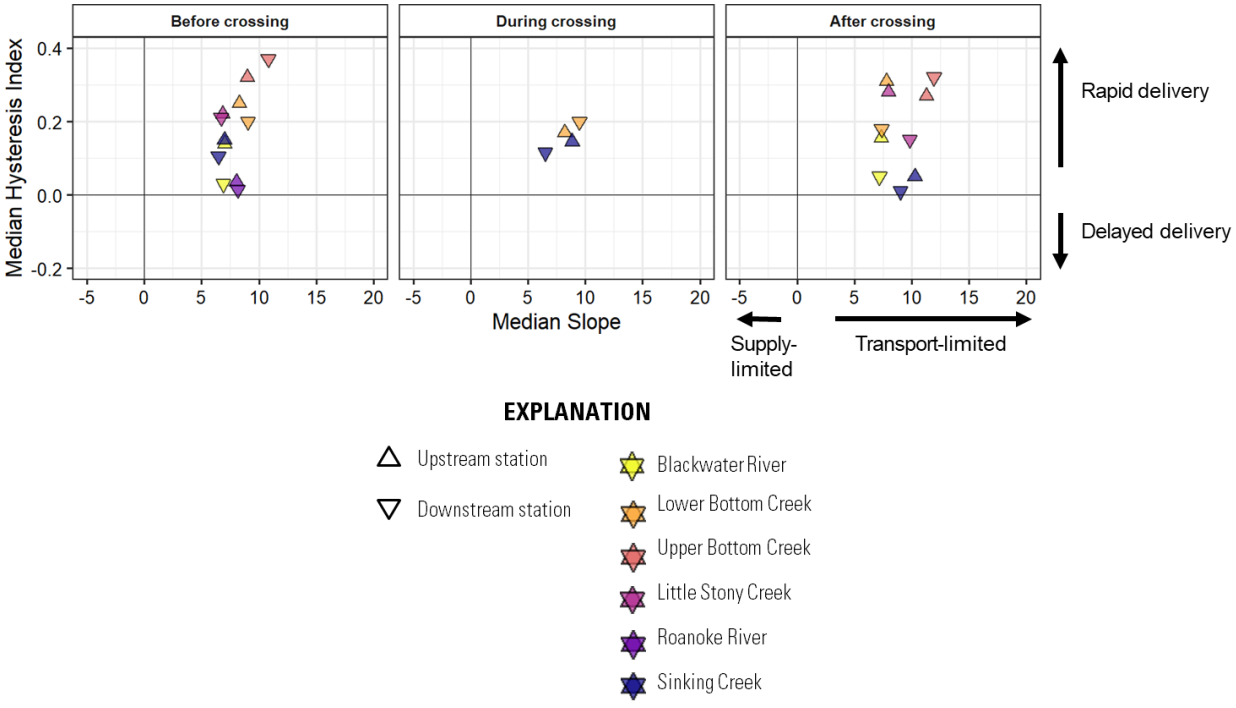

Figure 9. Graph showing the relations of median hysteresis index to median slope of the upstream and downstream site at all 6 crossing locations, *A,* Before Crossing; *B,* During Crossing; *C,* After Crossing. A positive median hysteresis index indicates rapid delivery and negative is delayed delivery. Positive median slope is transport-limited, and a negative median slope is supply limited.

Discussion of Turbidity Results

Turbidity analyses were conducted to evaluate whether pipeline stream crossing construction resulted in increased turbidity conditions during the crossing period relative to the turbidity regime measured using high-frequency data from sensors over the 7-year study period. Turbidity is a parameter of interest and importance due to its strong and well-established relation to suspended sediment concentration (Porter, 2025; Miller and others, 2023; Rügner and others, 2013; Stubblefield and others, 2007). Sedimentation has been associated with pipeline construction from crossings streams in previous studies (Moyer and Hyer, 2009; Lévesque and Dubé, 2007) and sedimentation has been shown to adversely affect in-stream biota and ecological functions (Henley and others, 2000; Wilber and Clarke, 2001). Measuring turbidity at a high frequency provided additional information about the short-term anomalous events observed. From US EPA (2003), of the 29 states that had a threshold for turbidity, 10 FNU was the most common threshold. Fifteen states set thresholds based on comparison to background conditions, 12 have absolute turbidity thresholds, and 2 use a combination of both, with most states having stricter thresholds for streams that support colder water aquatic communities. All observed median upstream-to-downstream differences in this study were less than established thresholds for turbidity for all states that have a statute for turbidity except for one state whose threshold is 0 FNU above background conditions.

Results from the analysis of the high-frequency turbidity data at all six stream crossing sites did not show evidence of long-term, persistent effects from pipeline crossing construction. Short-term, anomalously high turbidity conditions during stream crossing observed in this study were not of magnitude or duration sufficient to produce an upstream-to-downstream difference in median turbidity higher than established states thresholds or those needed to alter ecological

function. Across all sites, no significant difference in turbidity was observed between the before and after construction periods, which is consistent with similar studies in the region (Moyer and Hyer, 2009).

Storm turbidity hysteresis exhibited positive HI and positive slopes, indicating that most storms peak on the rising limb of hydrographs, which is consistent with similar studies (Waite and others, 2023; Lloyd and others, 2016a, Lloyd and others, 2016b; Fovet and others, 2018). The positive HI indicate rapid flushing from a proximal source. The results of the hysteresis analysis; however, generally show consistency between upstream and downstream stations at all sites and periods. The storm hysteresis patterns add to the body of evidence that no persistent changes in turbidity were identified.

Previous studies of pipeline stream crossings have primarily focused on comparing pipeline stream crossing methods at a single downstream station and have monitored suspended sediment concentration and total suspended solids (Lévesque and Dubé, 2007; Reid and others, 2002). However, these studies often have low sample collection frequency, are collected for a relatively short duration (less than 1 year), or do not monitor multiple crossings in the same study. However, Moyer and Hyer (2009) collected high-frequency turbidity data before, during, and after two pipeline stream crossings, which used two different crossing methods. Moyer and Hyer (2009) provided evidence that the trenchless crossing method had little effect on turbidity conditions; however, the largest magnitude anomalous turbidity observation observed in this study occurred at lower Bottom Creek, which was crossed using a trenchless crossing method. This might suggest that other potential factors might be driving these short-term anomalous conditions, such as ROW construction, failed sediment traps, high soil erosivity, or natural watershed processes like bank erosion. The median differences in Moyer and Hyer (2009) and in

the present report both generally showed low median turbidity differences between upstream and downstream stations across streams and periods.

Utility of Real-Time Alert Application

Out of the total 44,256,853 measurements from the USGS monitoring stations, a total of 137,263 (0.3-percent) flags were identified using the USGS real-time data when the parameter values exceeded parameter-specific water quality standards or thresholds (Table 8).

Table 8. Summary of the number of flags from January 2018 to June 2025 by field parameter using the real-time alert application.

[*, one flag indicates a 30-minute window of exceedance]

Field Parameter	Flag Name	Total count per flag	Total count per field parameter
Water Temperature (WT)	Upstream maximum	21,677	52,399
	Downstream maximum	19,995	
	Rise above natural	10,727	
Dissolved Oxygen (DO)	Upstream minimum	6,741	20,073
	Downstream minimum	9,032	
	Upstream-downstream difference	4,300	
pH	Upstream	19,725	42,179
	Downstream	5,298	
	Upstream-downstream difference	17,156	
Specific Conductance (SC)	Upstream maximum	77	283
	Downstream maximum	49	
	Upstream-downstream difference	3	
	Upstream-downstream percentage difference	154	
Turbidity (TB)*	Upstream-downstream exceedance*	5,700*	22,329*
	Upstream-downstream percentage exceedance*	4,602*	
	Upstream exceeds 99th percentile*	8,055*	
	Downstream exceeds 99th percentile*	3,972*	

Alerts could be caused by a flag from the real-time alert system, self-reported by MVP, or a reported field complaint. There were 464 total alerts produced from the real-time alert

application from January 2018 to June 2025 among all six crossing sites. Out of the 464 alert notices, 253 (55-percent) resulted in a compliance action and 211 (45-percent) resulted no compliance issues.

Application of the real-time alert system provided timely information about stream conditions, to regulators, installers, and the public, which can contribute to minimizing potential short- and long-term effects and improving regulatory agencies responses (Storey and others, 2011). Most of the real-time alerts resulted in compliance issues found on site, which likely would not have been identified without the alert system. Overall, the real-time alert system was beneficial for addressing and resolving compliance issues in a timely manner.

Summary

Construction of the nationwide natural gas pipeline network in the United States required crossing streams, rivers, and other waterbodies which are sources of drinking water and support sensitive aquatic biota and habitat. Stream crossings using both trenched or trenchless methods has the potential to alter the short-term or long-term water quality downstream. An excess of suspended sediments or warming water temperatures may reduce the water quality, degrade aesthetics, and impact the aquatic biota and habitat. The U.S. Geological Survey began a continuous monitoring program in 2017 to study the water quality changes from pre-construction background conditions through a year after the post-restoration of six sites upstream and downstream of construction. This report (1) presents the site-water temperature and turbidity data from all three monitored periods; (2) describes the potential for short- and long-term effects of pipeline crossing construction on varying sized watersheds; and (3) explains the results from

statistical testing of water temperature and turbidity; (4) identifies and explains water temperature anomaly testing; and (5) analyzes and explains storm hysteretic behavior.

The water temperature at all sites site ranged from -2 to 30.4 °C, with maximum temperatures in July and August and minimum temperatures in the January. The bootstrapped statistical tests of the median between the differences in water temperature upstream and water temperature downstream of pipeline crossings indicated that only Sinking Creek and upper Bottom Creek in the during period were statistically significant. At all sites, the bootstrapped upper and lower 99-percent confidence intervals were between 0 and 0.1 °C, which is less than the combined uncertainty of the instruments. Hourly median difference water temperature anomalies were used to identify differences in the time series with the removal of seasonal and long-term trends. Anomalies were identified in 0.95-percent of the data across all the sites (n = 7,284 of 766,504). All the downstream-warmer anomalies were less than or equal to 18 hours, with most of the events lasting 2 hours or less in duration (61-percent) for both upstream- and downstream-warmer anomalies. Most of the differences in the anomalies were small between upstream and downstream, with 63-percent of the downstream-warmer and 68-percent of the upstream warmer less than or equal to 1 °C. In general, the thermal regime between upstream and downstream was characterized by low frequency, short duration, and low magnitude anomalies consistently throughout the monitoring period, suggesting that changes in temperatures could not be solely attributed to pipeline crossing construction.

The turbidity at all sites ranged from 0 to greater than 1000 FNU and, in general, showed increasing turbidity with increased water-level. Bootstrapped statistical tests of the median between the differences in turbidity upstream and turbidity downstream of pipeline crossings indicated that there was no significant difference between the turbidity upstream and turbidity

downstream of the crossing. An evaluation of the median hysteresis index compared to median slope at each site suggests there was not a change in the timing of sediment delivery or rate of delivery during storms between the before and after periods. All sites and periods which were investigated had a positive median hysteresis index and a positive median slope. All sites were analyzed for hysteresis in the before and after period; Sinking Creek and lower Bottom Creek were the only streams analyzed in the during period due to a lack of storms captured at the other sites. A positive median slope indicated solute enrichment during a storm which is limited by the connectivity or transport capacity of the flow and a positive hysteresis index indicates that most of the sediment was moved on the rising limb of the hydrograph and there was a rapid flush of a proximal source. If there was excess sediment from pipeline construction, the median hysteresis index might have a change in HI, either more positive or negative, or had higher magnitude slopes. Some of the sites hysteresis index values were close to zero which could mean there was no hysteresis.

The real-time alert system was utilized by Virginia DEQ to identify potential compliance issues at all six crossings for water temperature, specific conductance, pH, dissolved oxygen, and turbidity. The alert flags were defined to identify measurements or differences between upstream and downstream measurements that fell below a minimum standard, exceeded a maximum standard, or exceeded a site-specific threshold. The alert system began in January of 2018. There was an alert 0.3-percent of the entire monitoring period and 464 total alert notices. An alert notice resulted in a site visit 81-percent of the time, a count of 374. When there was a notice, a compliance issue occurred 253 times, or 55-percent of the total times. The real-time alert system quickly identified and fixed compliance issues during pipeline construction. The use of a real-time alert system could minimize potential short- and long-term effects of pipeline construction.

There was no observed relation between crossing method (that is, trenched or trenchless) and in-stream turbidity or water temperature. Upper Bottom Creek and Blackwater River were crossed using trenched methods, and lower Bottom Creek, Sinking Creek, Little Stony Creek, and the Roanoke River were crossed using trenchless methods. There were no statistical differences in the median of turbidity differences or changes in the hysteretic behavior due to crossing method. There also were not consistent anomalies in the during crossing or after crossing period that could be attributed to crossing methodology that could not be attributed to short duration. The only effect that crossing method showed was the trenched sites had a shorter crossing period and therefore did not capture as much hydrologic variation as the before or after periods.

Findings from this multi-year study provide evidence that the pipeline crossing construction did not strongly affect water temperature or turbidity. The upstream-downstream comparative study observed some short-term anomalous water temperature and turbidity conditions but suggested overall water temperature and turbidity regimes over the entire monitoring period remained consistent. The synthesis of findings on six streams in mountainous southwestern Virginia did not suggest the pipeline construction significantly changed overall water temperature and turbidity regimes at the monitored locations. There is abundant utility for deploying real-time continuous monitors for construction. Regulatory agencies or other groups can utilize the real-time monitors to identify potential compliance issues immediately and work to investigate them and resolve any potential issues quickly. The real-time alert application for this study identified 464 number of potential compliance issues that were investigated by Virginia DEQ, of which 253 (55-percent) were successfully identified leading to an action.

References Cited

Alfonso, S., Gesto, M., and Sadoul, B., 2021, Temperature increase and its effects on fish stress physiology in the context of global warming: Journal of Fish Biology, v. 98, no. 6, p. 1496–1508, accessed July 30, 2025, at https://doi.org/10.1111/jfb.14599.

Baker, E.B., Showers, W.J., 2019, Hysteresis analysis of nitrate dynamics in the Neuse River, NC, Science of the Total Environment, v. 652, p. 889 – 899, accessed July 21, 2025, at https://doi.org/10.1016/j.scitotenv.2018.10.254.

Balkin, R.S., Lenz, S., 2021, Contemporary Issues in Reporting Statistical, Practical, and Clinical Significance in Counseling Research, Journal of Counseling and Development, v. 99, p. 227-237, accessed August 18, 2025, at https://doi.org/10.1002/jcad.12370.

Berger, E., Haase, P., Kuemmerlen, M., Leps, M., Schäfer, R.B., and Sundermann, A., 2017, Water quality variables and pollution sources shaping stream macroinvertebrate communities: Science of The Total Environment, v. 587–588, p. 1–10, accessed July 30, 2025, at https://doi.org/10.1016/j.scitotenv.2017.02.031.

Betcher, M., Hanna, A., Hansen, E., and Hirschman, D., 2019, Pipeline Impacts to Water Quality, 39 pp., accessed July 3, 2025, at https://www.tu.org/wp-content/uploads/2019/10/Pipeline-Water-Quality-Impacts-FINAL-8-21-2019.pdf.

Bonacina, L., Fasano, F., Mezzanotte, V., and Fornaroli, R., 2023, Effects of water temperature on freshwater macroinvertebrates: a systematic review: Biological Reviews, v. 98, no. 1, p. 191–221, accessed July 30, 2025, at https://doi.org/10.1111/brv.12903.

Burns, D.A., Pellerin, B.A., Miller, M.P., Capel, P.D., Tesoriero, A.J., Duncan, J.M., 2019, Monitoring the riverine pulse: Applying high-frequency nitrate data to advance integrative

understanding of biogeochemical and hydrological processes, WIREs Water, v. 6, no. 4, p. 13–48, https://doi.org/10.1002/wat2.1348.

Burton, J., Gerritsen, J., 2003, A Stream Condition Index for Virginia Non-Coastal Streams: Tetra Tech, Inc: 163 pp., accessed August 13, 2025, at https://www.deq.virginia.gov/home/showpublisheddocument/4317/637461491373170000.

Caissie, D., 2006, The thermal regime of rivers: a review: Freshwater Biology, v. 51, no. 8, p. 1389–1406, accessed July 21, 2025, at https://doi.org/10.1111/j.1365-2427.2006.01597.x.

Castro, J.M., MacDonald, A., Lynch, E., and Thorne, C.R., 2015, Risk-based Approach to Designing and Reviewing Pipeline Stream Crossings to Minimize Impacts to Aquatic Habitats and Species: River Research and Applications, v. 31, no. 6, p. 767–783, accessed June 27, 2025, at https://doi.org/10.1002/rra.2770.

Christensen, N. D., Czuba, J. A., Triantafillou, S., Copenheaver, C. A., Peterson, J. A., Hession, W. C., 2022, Establishment and persistence of trees growing in the channel of an intermittent stream in a temperate, karst environment. Water Resources Research, v. 58, no., e2021WR031528, 19 p., accessed August 23, 2025, at https://doi.org/10.1029/2021WR031528.

Coats, W.A., and Jackson, C.R., 2020, Riparian canopy openings on mountain streams: Landscape controls upon temperature increases within openings and cooling downstream: Hydrological Processes, v. 34, no. 8, p. 1966–1980, accessed July 3, 2025, at https://doi.org/10.1002/hyp.13706.

Dancho, M., and Vaughan, D., 2018, anomalize: Tidy Anomaly Detection: The R Foundation, accessed July 8, 2025, at https://doi.org/10.32614/cran.package.anomalize.

Dancho M, Vaughan D (2023). _anomalize: Tidy Anomaly Detection_. R package version 0.3.0, <https://CRAN.R-project.org/package=anomalize>.

Donaldson, M.R., Cooke, S.J., Patterson, D.A., and Macdonald, J.S., 2008, Cold shock and fish: Journal of Fish Biology, v. 73, no. 7, p. 1491–1530, accessed July 30, 2025, at https://doi.org/10.1111/j.1095-8649.2008.02061.x.

Downstream Strategies and West Virginia Rivers, 2024, Mountain Valley Pipeline Stream and Wetland Crossings: Review of Inspection Report, 15 pp., accessed July 4, 2025, at https://wvrivers.org/wp-content/uploads/2024/11/MVP-November-2024-Audit-Report.pdf.

Erickson, R.J., 1985, An evaluation of mathematical models for the effects of pH and temperature on ammonia toxicity to aquatic organisms: Water Research, v. 19, no. 8, p. 1047–1058, accessed July 30, 2025, at https://doi.org/10.1016/0043-1354(85)90375-6.

Fovet, O., Humbert, G., Dupas, R., Gascuel-Odoux, C., Gruau, G., Jaffrezic, A., Thelusma, G., Faucheux, M., Gilliet, N., Harmon, Y., Grimaldi, C., 2018, Seasonal variability of stream water quality response to storm events captured using high-frequency and multi-parameter data. Journal of Hydrology, v. 559, p. 282–293, accessed July 11, 2025, at https://doi.org/10.1016/j.jhydrol.2018.02.040.

Gendaszek, A.S., and Appel, M., 2022, Thermal heterogeneity and cold-water anomalies within the lower Yakima River, Yakima and Benton Counties, Washington: U.S. Geological Survey 2021–5140, accessed July 28, 2025, at Scientific Investigations Report, at https://doi.org/10.3133/sir20215140.

Gómez-de-Mariscal, E., Guerrero, V., Sneider, A, Jayatilaka, H., Phillip, J., Wirtz, D., Muñoz-Barrutia, A., 2021, Use of the p-values as a size-dependent function to address practical

differences when analyzing large datasets, c. 11, no. 20942, 15 p., accessed August 15, 2025, at https://doi.org/10.1038/s41598-021-00199-5.

Gowdy, M.J., Smits, M.P., Wilkey, P.L., and Miller, S.F., 1994, Data summary report on short-term turbidity monitoring of pipeline river crossings in the Moyie River, Boundary County, Idaho: PGT-PG&E Pipeline Expansion Project: Argonne National Lab., IL (United States) ANL/ESD/TM--67, accessed July 29, 2025, at https://doi.org/10.2172/10161518.

Henley, W. F., Patterson, M. A., Neves, R. J., & Lemly, A. D., 2000, Effects of Sedimentation and Turbidity on Lotic Food Webs: A Concise Review for Natural Resource Managers. Reviews in Fisheries Science, v. 8, no. 2, p. 125–139, accessed August 17, 2025 at https://doi.org/10.1080/10641260091129198.

Honious, S. A., S., Hale, R. L., Guilinger, J. J., Crosby, B. T., & Baxter Colden, V., 2022, Turbidity structures the controls of ecosystem metabolism and associated metabolic process domains along a 75-km segment of a semiarid stream. Ecosystems, v. 25, no. 2, p. 422-440, accessed August 17, 2025 at, https://doi.org/10.1007/s10021-021-00661-5.

Houser, D.L., and Pruess, H., 2009, The effects of construction on water quality: a case study of the culverting of Abram Creek: Environmental Monitoring and Assessment, v. 155, no. 1, p. 431–442, accessed July 22, 2025, at https://doi.org/10.1007/s10661-008-0445-9.

Huenemann, T. W., Dibble, E. D., & Fleming, J. P., 2012, Influence of Turbidity on the Foraging of Largemouth Bass. Transactions of the American Fisheries Society, v. 141, no. 1, p. 107–111, accessed August 17, 2025, at https://doi.org/10.1080/00028487.2011.651554.

Jamshidi, E.J., Yusup, Y., Kayode, J.S., and Kamaruddin, M.A., 2022, Detecting outliers in a univariate time series dataset using unsupervised combined statistical methods: A case study

on surface water temperature: Ecological Informatics, v. 69, p. 101672, accessed July 17, 2025, at https://doi.org/10.1016/j.ecoinf.2022.101672.

The Joint Committee for Guides in Metrology (JCGM), 2020, Guide to the expression of uncertainty in measurement — Part 6: Developing and using measurement models, accessed August 17, 2025, at https://www.bipm.org/documents/20126/2071204/JCGM_GUM_6_2020.pdf/d4e77d99-3870-0908-ff37-c1b6a230a337.

Johnson, M.F., Albertson, L.K., Algar, A.C., Dugdale, S.J., Edwards, P., England, J., Gibbins, C., Kazama, S., Komori, D., MacColl, A.D.C., Scholl, E.A., Wilby, R.L., de Oliveira Roque, F., and Wood, P.J., 2024, Rising water temperature in rivers: Ecological impacts and future resilience: WIREs Water, v. 11, no. 4, p. e1724, accessed July 30, 2025, at https://doi.org/10.1002/wat2.1724.

Johnston, M.G., Faulkner, C., 2021, A bootstrap approach is a superior statistical method for the comparison of non-normal data with differing variance, The New Phytologist, v. 230, no. 1, p. 23–26, accessed July 21 2025, at https://www.jstor.org/stable/10.2307/27001227.

Knapp, J. L., von Freyberg, J., Studer, B., Kiewiet, L., Kirchner, J., 2020, Concentration-discharge relationships vary among hydrological events, reflecting differences in event characteristics, Hydrology and Earth System Sciences Discussions, v. 24, no. 5, p. 1–27, accessed August 1, 2025, at https://doi.org/10.5194/hess-2019-684.

Krawczyk, M., 2015, The Search for Significance: A Few Peculiarities in the Distribution of P Values in Experimental Psychology Literature, PLoS ONE, v. 10, no. 6, e0127872 p., accessed August 14, 2025, at https://doi.org/10.1371/journal.pone.0127872.

Leach, J.A., Kelleher, C., Kurylyk, B.L., Moore, R.D., and Neilson, B.T., 2023, A primer on stream temperature processes: WIREs Water, v. 10, no. 4, p. e1643, accessed July 30, 2025, at https://doi.org/10.1002/wat2.1643.

Lévesque, L.M., and Dubé, M.G., 2007, Review of the effects of in-stream pipeline crossing construction on aquatic ecosystems and examination of Canadian methodologies for impact assessment: Environmental Monitoring and Assessment, v. 132, no. 1, p. 395–409, accessed July 27, 2025, at https://doi.org/10.1007/s10661-006-9542-9.

Lin, M.,, Lucas, H.C. jr., Shmueli, G., 2013, Too Big to Fail: Large Samples and the p-Value Problem, Information Systems Research, p. 1-12, accessed August 14, 2025, at http://dx.doi.org/10.1287/isre.2013.0480.

Liu, W., Birgand, F., Tian, S., Chen, C., 2021, Event-scale hysteresis metrics to reveal processes and mechanisms controlling constituent export from watersheds: A review, Water Research, v. 200, no. 117254, p. 1–13, accessed June 11, 2025, at https://doi.org/10.1016/j.watres.2021.117254.

Lloyd, C. E. M. and Freer, J. E. and Johnes, P. J. and Collins, A. L., 2016a, Technical Note: Testing an improved index for analyzing storm discharge--concentration hysteresis, Hydrology and Earth System Sciences, v. 20, no. 2, p. 625–632, accessed June 10, 2025, at https://doi.org/10.5194/hess-20-625-2016.

Lloyd, C. E. M., Freer, J. E., Johnes, P. J., Collines, A. L., 2016b, Using hysteresis analysis of high-resolution water quality monitoring data, including uncertainty, to infer controls on nutrient and sediment transfer in catchments, Science of the Total Environment, v. 543, no. A, p. 388–404, accessed July 21, 2025, at http://dx.doi.org/10.1016/j.scitotenv.2015.11.028.

Mejia, F.H., Torgersen, C.E., Berntsen, E.K., Maroney, J.R., Connor, J.M., Fullerton, A.H., Ebersole, J.L., and Lorang, M.S., 2020, Longitudinal, Lateral, Vertical, and Temporal Thermal Heterogeneity in a Large Impounded River: Implications for Cold-Water Refuges: Remote Sensing, v. 12, no. 9, p. 1386, accessed July 31, 2025, at https://doi.org/10.3390/rs12091386.

Millar, D., Buda, A., Duncan, J., Kennedy, C., 2022, An open-source automated workflow to delineate storm events and evaluate concentration-discharge relationships, Hydrol. Process., v. 36, no. 1, p. 1–12, accessed June 10, 2025, at https://doi.org/10.1002/hyp.14456.

Miller, S. A., Webber, J. S., Jastram, J. D., Aguilar, M. F., 2023, Using high-frequency monitoring data to quantify city-wide suspended-sediment load and evaluate TMDL goals. Environmental Monitoring and Assessment, v. 195, no. 11, p. 1–21, https://doi.org/10.1007/s10661-023-11905-3.

Morrill, J.C., Bales, R.C., and Conklin, M.H., 2005, Estimating Stream Temperature from Air Temperature: Implications for Future Water Quality: Journal of Environmental Engineering, v. 131, no. 1, p. 139–146, accessed on August 17, 2025, at https://doi.org/10.1061/(ASCE)0733-9372(2005)131:1(139).

Moyer, D.L., and Hyer, K.E., 2009, Continuous turbidity monitoring in the Indian Creek watershed, Tazewell County, Virginia, 2006–08: U.S. Geological Survey Scientific Investigations Report 2009–5085, 42 p.

Mudelsee, M., Alkio, M., 2007, Quantifying effects in two-sample environmental experiments using bootstrap confidence intervals, Environmental Modelling and Software, v. 22, no. 1, p. 84–96, accessed August 1, 2025, at https://doi.org/10.1016/j.envsoft.2005.12.001.

Musolff, A., Zhan, Q., Dupas, R., Minaudo, C., Fleckenstein, J. H., Rode, M., Dehaspe, J., Rinke, K., 2021, Spatial and temporal variability in concentration discharge relationships at the

event scale. Water Resources Research, v. 57, no. e2020WR029442, p. 1–21, accessed, June 10, 2025, at https://doi.org/10.1029/2020WR029442.

New Jersey Department Of Environmental Protection, 2021, Horizontal Directional Drilling, 25 pp., accessed June 27, 2025.

New River Geographics, LLC, 2017, Mountain Valley Pipeline - A Comprehensive Story Map: accessed August 8, 2025, at https://data-nrgeo.opendata.arcgis.com/apps/mountain-valley-pipeline-a-comprehensive-story-map/explore.

Noyes, P.D., and Lema, S.C., 2015, Forecasting the impacts of chemical pollution and climate change interactions on the health of wildlife: Current Zoology, v. 61, no. 4, p. 669–689, accessed July 30, 2025, at https://doi.org/10.1093/czoolo/61.4.669.

Parfomak, P.W., and Vann, A., 2022, Mountain Valley Pipeline: Permitting Issues: Congressional Research Service IN12032, 3 pp., accessed June 24, 2025, at https://www.congress.gov/crs_external_products/IN/PDF/IN12032/IN12032.1.pdf.

Parfomak, P.W., and Vann, A., 2024, Mountain Valley Pipeline: Past the Finish Line, 3 pp., accessed June 24, 2025, at https://www.congress.gov/crs_external_products/IN/PDF/IN12032/IN12032.14.pdf.

Porter, A., 2025, Spatiotemporal patterns in urban nutrient and suspended sediment loads and stream response to watershed management implementation, Environmental Monitoring and assessment, v. 197, no. 497, p. 1-26, accessed August 3, 2025, at https://doi.org/10.1007/s10661-025-13917-7.

R Core Team, 2025, R—A language and environment for statistical computing. R Foundation for Statistical Computing software release, accessed June 2, 2025, at https://www.R-project.org/.

Reed, M., 2024, North America 2024 Pipeline Construction Outlook: New LNG Terminals Lead Call for More Pipelines: Underground Infrastructure, v. 79, accessed August 14, 2025, at, https://undergroundinfrastructure.com/magazine/2024/february-2024-vol-79-no-2/features/north-america-2024-pipeline-construction-outlook-new-lng-terminals-lead-call-for-more-pipelines.

Reid, S.M., Stoklosar, S., Metikosh, S., and Evans, J., 2002, Effectiveness of Isolated Pipeline Crossing Techniques to Mitigate Sediment Impacts on Brook Trout Streams: Water Quality Research Journal, v. 37, no. 2, p. 473–488, accessed June 27, 2025, at https://doi.org/10.2166/wqrj.2002.031.

Roanoke Weather Records, 2025, accessed August 8, 2025 at https://www.extremeweatherwatch.com/cities/roanoke.

Rügner, H., Schwientek, M., Beckingham, B., Kuch, B., Grathwohl, P., 2013, Turbidity as a proxy for total suspended solids (TSS) and particle facilitated pollutant transport in catchments, Environmental Earth Sciences, v. 69, p. 373 – 380, accessed August 4, 2025, at https://doi.org/10.1007/s12665-013-2307-1.

Sauer, V.B., and Turnipseed, D.P., 2010, Stage measurement at gaging stations: U.S. Geological Survey Techniques and Methods book 3, chap. A7, 45 p.

Shikwambana, L., and Kganyago, M., 2023, Seasonal Comparison of the Wildfire Emissions in Southern African Region during the Strong ENSO Events of 2010/11 and 2015/16 Using Trend Analysis and Anomaly Detection: Remote Sensing, v. 15, no. 4, p. 1073, accessed July 08, 2025, at https://doi.org/10.3390/rs15041073.

Siegel, J.E., and Volk, C.J., 2019, Accurate spatiotemporal predictions of daily stream temperature from statistical models accounting for interactions between climate and landscape: PeerJ, v. 7, accessed on August 17, 2025, at https://doi.org/10.7717/peerj.7892.

Storey, M.V., van der Gaag, B., and Burns, B.P., 2011, Advances in on-line drinking water quality monitoring and early warning systems: Water Research, v. 45, no. 2, p. 741–747, accessed August 02, 2025, at https://doi.org/10.1016/j.watres.2010.08.049.

Stubblefield, A.P., Reuter, J.E., Dahlgren, R.A., Goldman, C.R., 2007, Use of turbidometry to characterize suspended sediment and phosphorus fluxes in the Lake Tahoe basin, California, USA, Hydrological Processes, v. 21, no. 3, p. 281–291, accessed August 1, 2025, at https://doi.org/10.1002/hyp.6234.

Tassone, S.J., Besterman, A.F., Buelo, C.D., Ha, D.T., Walter, J.A., and Pace, M.L., 2023, Increasing heatwave frequency in streams and rivers of the United States: Limnology and Oceanography Letters, v. 8, no. 2, p. 295–304, accessed on August 17, 2025, at https://doi.org/10.1002/lol2.10284.

Tetra Tech, 2021, Mountain Valley Pipeline Project Individual Permit Application: USACE Individual Permit Application, 107 pp., accessed June 24, 2025, at https://www.mountainvalleypipeline.info/wp-content/uploads/2021/03/aa_Individual-Permit-Application-Text-and-Tables_PUBLIC.pdf.

Turner, M.G., Pearson, S.M., Bolstad, P., and Wear, D.N., 2003, Effects of land-cover change on spatial pattern of forest communities in the Southern Appalachian Mountains (USA): Landscape Ecology, v. 18, no. 5, p. 449–464, accessed July 3, 2025, at https://doi.org/10.1023/A:1026033116193.

U.S. Energy Information Administration, 2024a, Natural gas explained: Natural gas pipelines, accessed August 14, 2025 at https://www.eia.gov/energyexplained/natural-gas/natural-gas-pipelines.php.

U.S. Energy Information Administration, 2024b, Natural gas explained: Use of natural gas, accessed August 14, 2025 at https://www.eia.gov/energyexplained/natural-gas/natural-gas-pipelines.php.

U.S. Energy Information Administration, 2025, Virginia: State Profile and Energy Estimates: accessed July 2, 2025, at https://www.eia.gov/state/?sid=VA#tabs-5.

U.S. Environmental Protection Agency, 2003, Developing water quality criteria for suspended and bedded sediments (SABS): Potential Approaches, DRAFT, accessed August 18, 2025 , at https://assessments.epa.gov/risk/document/&deid=164423#downloads.

U.S. Geological Survey, 2019, The StreamStats program, online at https://streamstats.usgs.gov/ss/, accessed on June 10, 2025.

U.S. Geological Survey, 2025a, National Geologic Map Database, accessed August 18, 2025, at https://ngmdb.usgs.gov/Geolex/stratres/provinces.

U.S. Geological Survey, 2025b, USGS water data for the Nation: U.S. Geological Survey National Water Information System database, accessed June 2025 at http://dx.doi.org/10.5066/F7P55KJN.

van Hamel, A., and Brunner, M.I., 2024, Trends and Drivers of Water Temperature Extremes in Mountain Rivers: Water Resources Research, v. 60, no. 10, p. e2024WR037518, accessed July 8, 2025, at https://doi.org/10.1029/2024WR037518.

Verheyen, J., Delnat, V., and Theys, C., 2022, Daily temperature fluctuations can magnify the toxicity of pesticides: Current Opinion in Insect Science, v. 51, p. 100919, accessed July 30, 2025, at https://doi.org/10.1016/j.cois.2022.100919.

Virginia Administrative Code. 9VAC25-260-50. Numerical criteria for dissolved oxygen, pH, and maximum temperature. Title 9, Agency 25, Chapter 250, Section 50. Accessed August 5, 2025, available at: https://law.lis.virginia.gov/admincode/title9/agency25/chapter260/section50/.

Virginia Administrative Code. 9VAC25-260-30. Antidegradation policy. Title 9, Agency 25, Chapter 260, Section 30. Accessed August 13, 2025, at https://law.lis.virginia.gov/admincode/title9/agency25/chapter260/section30/.

Virginia Department of Conservation and Recreation, 2021, The Natural Communities of Virginia Classification of Ecological Groups and Community Types, accessed August 13, 2025, at /www.dcr.virginia.gov/natural-heritage/natural-communities/ncta1

Wagner, R.J., Boulger, R.W., Jr., Oblinger, C.J., and Smith, B.A., 2006, Guidelines and standard procedures for continuous water-quality monitors—Station operation, record computation, and data reporting: U.S. Geological Survey Techniques and Methods 1–D3, 51 p. + 8 attachments; accessed April 10, 2006, at http://pubs.water.usgs.gov/tm1d3.

Waite, T., Jankowski, K. J., Bruesewitz, D. A., Van Appledorn, M., Johnston, M., Houser, J. N., Baumann, D., A., Bennie, B., 2023, River geomorphology affects biogeochemical responses to hydrologic events in a large river ecosystem. Water Resources Research, v. 59, no. e2022WR033662, p. 1–20, accessed July 1, 2025, at https://doi.org/10.1029/2022WR033662.

Wasko, C., Guo, D., 2022, Understanding event runoff coefficient variability across Australia using the hydroEvents R package. Hydrol. Process., v. 36, no.4, p. 1–14, accessed June 2, 2025, at https://doi.org/10.1002/hyp.14563.

Wilber, D.H., Clarke, D.G., 2001, Biological Effects of Suspended Sediments: A Review of Suspended Sediment Impacts on Fish and Shellfish with Relation to Dredging Activities in Estuaries, North American Journal of Fisheries Management, v. 21, p. 855-875 accessed August 18, 2025, at https://doi.org/10.1577/1548-8675(2001)021<0855:BEOSSA>2.0.CO;2.

Yan, X., Ariaratnam, S.T., Dong, S., and Zeng, C., 2018, Horizontal directional drilling: State-of-the-art review of theory and applications: Tunnelling and Underground Space Technology, v. 72, p. 162–173, accessed July 30, 2025, at https://doi.org/10.1016/j.tust.2017.10.005.

YSI, 2012, 6-series multiparameter water quality sondes: Yellow Springs Incorporated, 379 p, accessed August 13, 2025, at ysi.com/file library/documents/manuals/069300-ysi-6-series-manual-revj.pdf.

Zerga, B., 2024, Karst topography: Formation, processes, characteristics, landforms, degradation and restoration: A systematic review: Watershed Ecology and the Environment, v. 6, p. 252–269, accessed July 3, 2025, at https://doi.org/10.1016/j.wsee.2024.10.003.

Appendix 1. Supporting Material for Turbidity Analysis

This section is used to provide supplemental information for turbidity analysis and results.

Table 1.1. Number and percentage (%) of values censored that were greater than 1000 Formazin Nephelometric Units (FNU; U.S. Geological Survey, 2025b).

Paired Site Name	U.S. Geological Survey Site Number	Number of 5-min data points greater than 1000 FNU	Total number of 5-min turbidity data points collected	Percentage (%)
Little Stony Creek upstream	03171597	9	761,913	0.001
Little Stony Creek downstream	0317159760	235	725,683	0.032
Sinking Creek upstream	0317154954	0	697,630	0.000
Sinking Creek downstream	0317155123	6	727,344	0.001
Roanoke River upstream	0205450393	34	749,359	0.005
Roanoke River downstream	0205450495	294	750,045	0.039
Upper Bottom Creek upstream	0205373035	0	729,865	0.000
Upper Bottom Creek downstream	0205373075	0	750,858	0.000
Lower Bottom Creek upstream	0205373228	1	754,568	0.000
Lower Bottom Creek downstream	0205373422	0	727,498	0.000
Blackwater River upstream	0205696042	893	690,453	0.129
Blackwater River downstream	0205696095	942	666,465	0.141

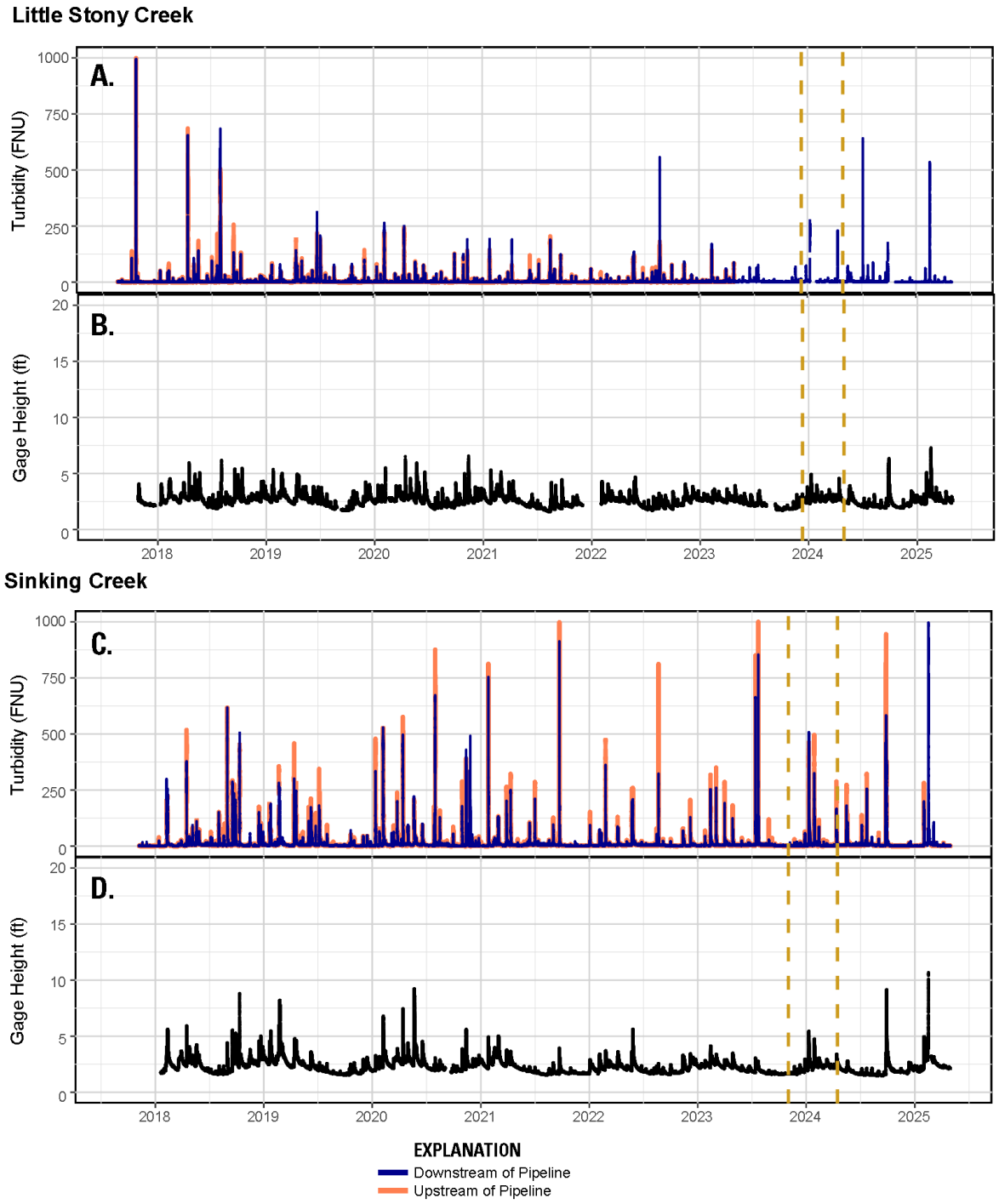

Figure 1.1. High-frequency time series of the before crossing, during crossing, and after crossing period. *A,* Little Stony Creek turbidity at the upstream and downstream site; *B,* Gage height at Little Stony Creek downstream site; *C,* Sinking Creek turbidity (in Formazin Nephelometric Units, FNU) at the upstream and downstream site; *D,* gage height at Sinking Creek upstream site.

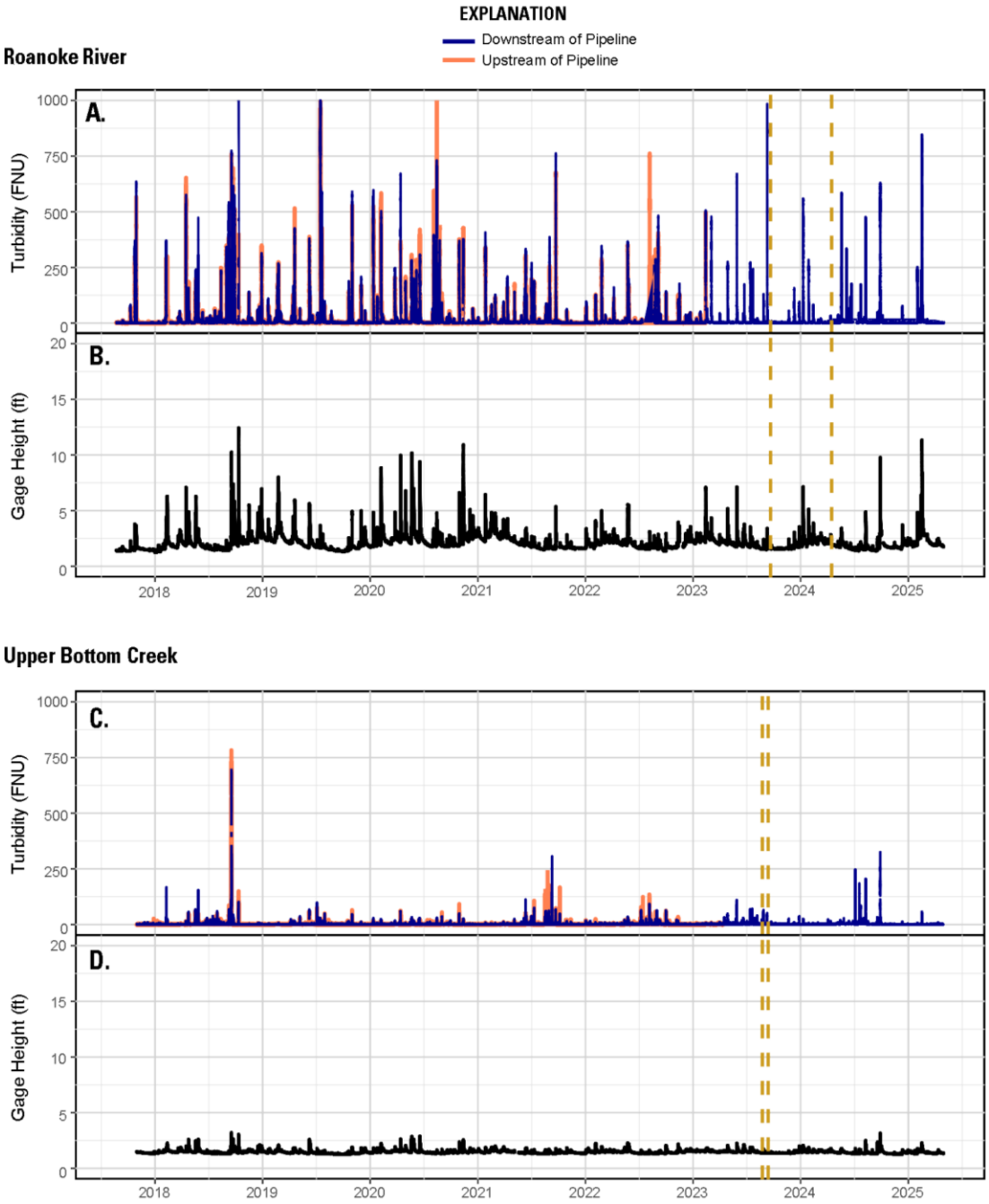

Figure 1.2. High-frequency time series of the before crossing, during crossing, and after crossing period. *A,* Roanoke River turbidity (in Formazin Nephelometric Units, FNU) at the upstream and downstream site; *B,* gage height at Roanoke River Lafayette monitoring station upstream of upstream site; *C,* upper Bottom Creek turbidity at the upstream and downstream site; *D,* gage height at upper Bottom Creek downstream site.

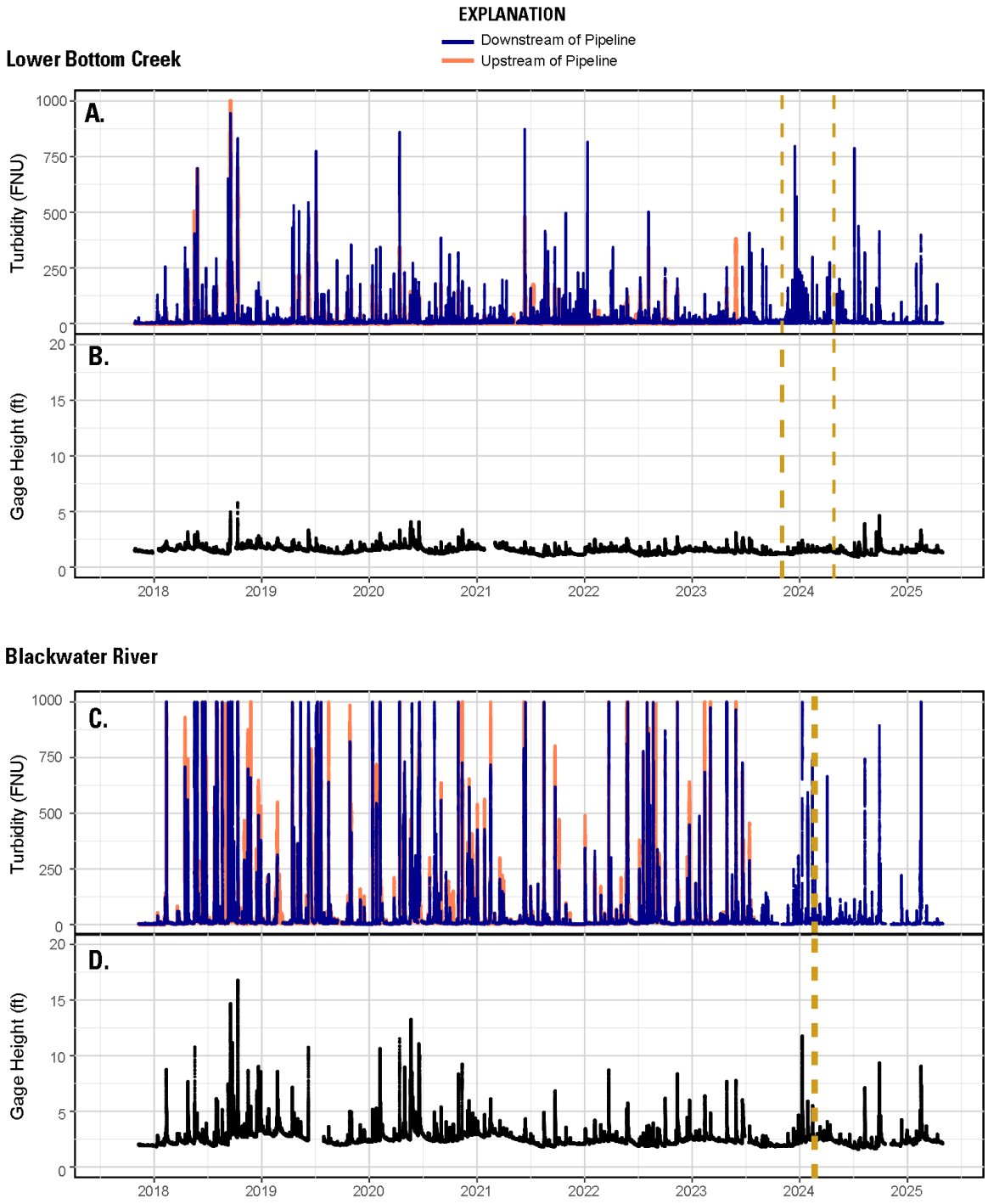

Figure 1.3. High-frequency time series of the before crossing, during crossing, and after crossing period. *A,* lower Bottom Creek turbidity (in Formazin Nephelometric Units, FNU) at the upstream and downstream site; *B,* gage height at lower Bottom Creek in the downstream site; *C,* Blackwater River turbidity at the upstream and downstream site; *D,* gage height at Blackwater River downstream site.

Table 1.2. Results of the percentage of absolute differences for each time-matched paired hourly median turbidity measurements between the upstream and downstream for each site and period.

Location	Period	N	Percent of absolute differences less than or equal to					Percent absolute differences greater than 100 FNU
			1 FNU	2 FNU	5 FNU	10 FNU	25 FNU	
Little Stony Creek	Before	50,713	91.2	97.6	99.3	99.7	99.9	0
	During	2,571	61.0	96.8	98.9	99.7	99.9	0
	After	7,419	89.5	98.1	99.5	99.7	99.9	0
Sinking Creek	Before	45,402	67.1	87.5	96.0	98.0	99.2	0
	During	3,705	71.0	86.7	96.7	98.6	99.5	0
	After	7,189	77.2	93.0	97.6	98.4	99.2	0.1
Roanoke River	Before	46,785	75.9	88.7	95.5	97.6	99.1	0
	During	4,405	86.6	95.0	98.1	99.2	99.9	0
	After	8,321	78.9	90.3	95.2	97.2	99.2	0.1
Upper Bottom Creek	Before	48,057	91.9	98.0	99.3	99.7	99.9	0
	During	501	57.9	93.6	96.8	98.2	99.6	0
	After	11,350	77.5	94.9	99.0	99.6	99.9	0
Lower Bottom Creek	Before	48,918	28.7	61.5	90.1	96.0	98.6	0.2
	During	3,804	31.3	51.7	79.7	89.1	95.5	0.4
	After	7,789	52.8	78.0	91.8	95.4	98.3	0.1
Blackwater River	Before	45,624	53.5	74.2	85.7	90.8	95.0	0.8
	During	286	31.8	64.7	89.2	93.7	97.2	0
	After	7,323	62.3	78.8	90.4	95.2	97.5	0.2

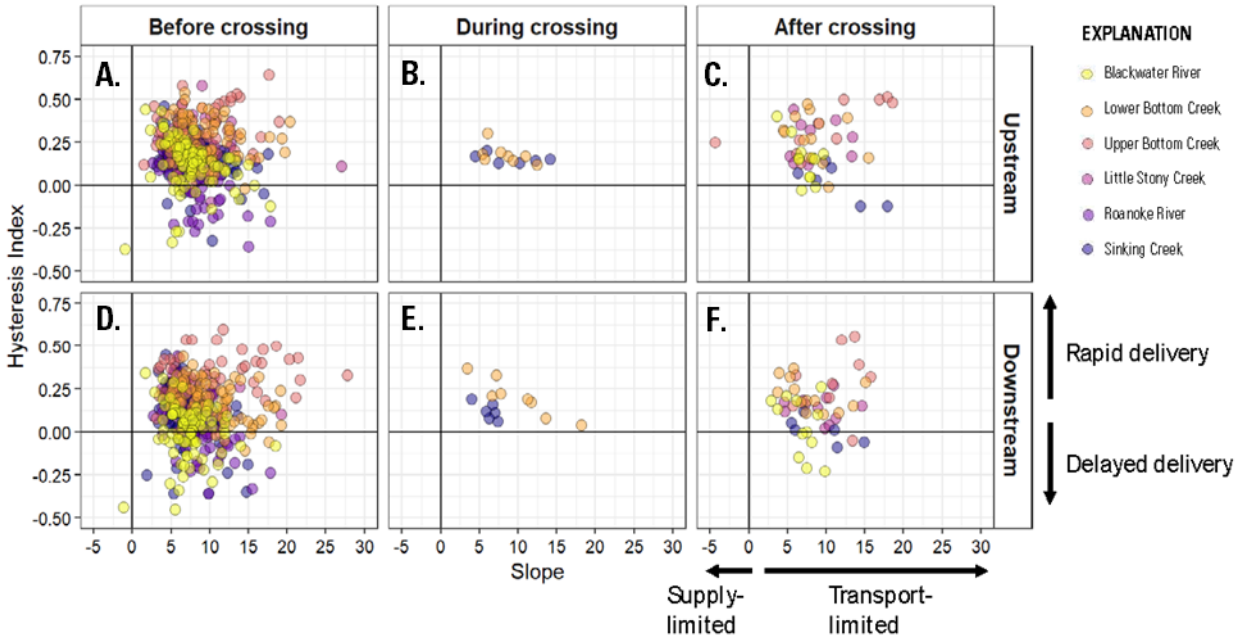

Figure 1.4. Graphs of the hysteresis index and slope. *A,* before crossing at upstream Sites; *B,* during crossing at upstream sites; *C,* after crossing at upstream sites; *D,* before crossing at downstream sites; *E,* during crossing at downstream Sites; *F,* after crossing at downstream sites.